國立臺灣大學工學院環境工程學研究所

碩士論文

Graduate Institute of Environmental Engineering

College of Engineering

National Taiwan University

Master Thesis

奈米薄膜對水中新興污染物的去除機制與模式探討

Elucidation of Rejection Mechanisms and Models for PPCPs/EDCs in aqueous solution by Nanofiltration Membrane

吳海翔

Hai-Hsiang Wu

指導教授：蔣本基教授

Advisor: Prof. Pen-Chi Chiang

中華民國 102 年 6 月

June, 2013

國立臺灣大學碩士學位論文
口試委員會審定書

奈米薄膜對水中新興污染物的去除機制與模式探討

Elucidation of Rejection Mechanisms and Models for PPCPs/EDCs in Aqueous Solution by Nanofiltration Membrane

本論文係吳海翔君(學號 r00541102)在國立臺灣大學環境工程學研究所完成之碩士學位論文，於民國一百零二年六月十三日承下列考試委員審查通過及口試及格，特此證明

論文審查委員：

顧 洋教授
國立台灣科技大學化學工程系

曾迪華教授
國立中央大學環境工程研究所

張怡怡教授
台北醫學大學醫學系生化學科

指導教授：

所　　長：

誌謝

本論文能順利完成，首先要感謝指導教授蔣本基教授的悉心指導與關懷，感謝張怡怡教授、顧洋教授、曾迪華教授在百忙之中參與口試並對論文的諸多指導與建議，使本論文更臻完善。也感謝黃金寶教授和田慶中教授，在有限的時間內對學生論文的內容及英文文法的諸多指教。在此由衷的感謝各位師長們。

在此要謝謝實驗室的夥伴們!謝謝仲暉學長，在我論文方向與協助我看論文時幫助許多，也在我討論實驗結果方面給我許多指導。謝謝親切的書弘，讓我能認識很多人，我們也一起經歷過許多事情。謝謝騰霆，我們一起在單操做實驗、互相幫助、一起奮鬥。謝謝可欣，一起在實驗室聊天，一起出遊。謝謝學弟晨晏，讓我有很多機會能教導，教學相長，將經驗傳承，我們也常一起聊天。謝謝實驗室的其他夥伴永惇學姊、國凱學長、則綸學長、意雯學姊、雅婷、冠薇學妹、偉勵學弟、溫翔學弟、交換生楊柳含子、子旭、柱堅，在期間給予的幫助、討論及聊天。

也要謝謝其他的朋友們!謝謝碩二的朋友們，懷念在 105 的一起奮鬥的時光，還有一起吃飯、出遊、聊天、玩遊戲，謝謝你們!謝謝我的室友俊傑、詠恩、舜歆，輪流做早餐，一起分享、禱告，也常容忍我較亂的環境。謝謝倍加團契的人，一起參與許多事，為我禱告!謝謝校園團契研究生小組的人，一起查經、吃飯、出遊、聊天，為我禱告。謝謝環工小排的人，在週五中午一起吃午餐、讀聖經、分享與禱告。

最後也要謝謝我的爸爸、媽媽和姊姊，從我小時候一直以來的照顧，讓我能成長獨立，雖然研究所因為較忙而較少回家，但謝謝你們的關心與包容!也感謝神，讓我能順利完成這本論文!

海翔謹致

2013 年 7 月

Abstract

The rejection mechanism of nine PPCPs/EDCs by nanofiltration membrane was systematically studied. Target compounds were classified into three groups: Group 1 (G1) was hydrophilic neutral compounds; Group 2 (G2) was negatively charged compounds; Group 3 (G3) was hydrophobic neutral compounds. To distinguish electrostatic repulsion, filtration experiments were conducted at pH 3 and pH 8. To differentiate adsorption effect, initial rejection and final rejection were compared. Adsorption experiment was conducted to validate the effect of adsorption.

The effect of membrane characteristic and operating condition on rejection was evaluated. The decrease in membrane pore radius significantly increased the rejection, whereas the increase in membrane thickness only slightly increased the rejection. Rejection increased as the transmembrane pressure increased, whereas rejection slightly increased and reach stable rejection as cross flow velocity increased.

The rejections of G1 solutes increased as the solute size (or molar weight) increased. The rejections of G1 and G3 solutes have almost the same at pH 8 and at pH 3, except for trimethoprim. However, the rejections of G2 solutes were higher at pH 8 than at pH 3 due to electrostatic repulsion. G3 solutes had adsorption effect, and the initial rejections were higher than the final rejection and decreased in the feed concentration

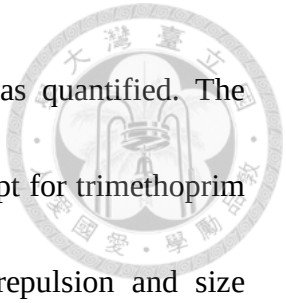

with time. The contribution of the three rejection mechanisms was quantified. The rejections of G1 solutes were governed only by size exclusion, except for trimethoprim at pH 3. The rejections of G2 were governed by electrostatic repulsion and size exclusion at pH 8. The rejections of G3 solutes were governed by adsorption and size exclusion.

The irreversible thermodynamics model and the extended Nerst-Planck model were used to predict rejection. The predicted rejection is more accurate for relatively small and medium compounds. However, it is overestimated for relatively larger compounds. The deviation may cause by the non-uniform of the membrane pore size. By comparing the effect of the cross flow velocity and the transmembrane pressure on predicted rejections and experimental rejections, results showed that the concentration polarization factor may play a role on rejection, but the value of the concentration polarization factor may not be calculated correctly.

Keywords: Nanofiltration membrane; Pharmaceutical and personal care products; Rejection mechanism; Endocrine disruptor chemicals; size exclusion; electrostatic repulsion; adsorption; rejection model.

摘要

本研究使用九種個人保健藥品(PPCPs)或內分泌干擾物質(EDCs)來系統化的研究奈米薄膜(NF)的去除機制。目標化合物被分成三組：第一組(G1)為親水性中性物質；第二組(G2)為帶負電物質；第三組(G3)為疏水性中性物質。為了要區分電荷斥力的效果，奈米薄膜過濾實驗在 pH 3 和 pH 8 的條件下進行。而區分吸附的效果，奈米薄膜過濾實驗初始的去除率和最終去除率比較。

本研究評估薄膜特性與操作條件對去除率的影響。薄膜孔徑的減少會顯著的增加去除率，而薄膜厚度的增加會少量的增加去除率。透膜壓力的增加會使去除率呈線性上升，而增加掃流速度使去除率先上升接著達到穩定的去除率。

G1 化合物去除率隨著溶質大小(分子量)的增加而增加。G1 和 G3 在 pH 8 和 pH 3 的去除率的差距不顯著，但 G2 在 pH 8 的去除率比 pH 3 來得高，原因為電荷斥力作用。G3 化合物由於有吸附作用，濃度與去除率會隨著時間降低，且最終的去除率可能會低於相似大小的 G1。本研究中定量三個去除機制對去除率的貢獻，結果顯示 G1 的去除率僅由分子篩除所控制，但在 pH 3 trimethoprim 有電荷斥力作用；G2 的去除率由電荷斥力和分子篩除所控制；G3 的去除率由分子篩除和吸附所控制。

本研究使用 Irreversible thermodynamics 及 extended Nerst-Planck 模式來預測去除率。預測結果在小分子情況下較為準確，大分子則有高估情況。改變掃流速度與透膜壓力會改變濃度極化因子，雖然濃度極化因子對於去除率是有影響，但是其數值很可能有估算錯誤的情況，因而造成去除率的估算有誤差。

關鍵字：奈米薄膜；去除機制；個人保健藥物(PPCPs)；內分泌干擾物質(EDCs)；分子篩除;電荷斥力；吸附；去除模式。

Content

List of Figure

List of Table

Oral Defense Comments

顧洋教授：

	疑問與建議	回覆
1	名詞 Solvent flux 和 permeate flux 是同一個嗎? 模式公式似乎不一致	謝謝教授的建議，已統一改成 solvent flux 模式公式確認
2	濃度極化現象的對溶質去除率的影響?如何解釋? 掃流速度有做 0.09~0.27 m/s，為何不再往低流速進行實驗?如何判斷掃流速度的影響?	謝謝教授的問題， 掃流速度與濃度極化現象的影響在 4-1-3 節有說明。 低流速的實驗不易進行因此沒做。
3	吸附現象與 log Kow 的關係為何?為何 log Kow 2.5 時無吸附效果，但 3.5 時有吸附效果? 薄膜的親疏水性為何	謝謝教授的問題， 吸附的影響在 4-2-3 節有說明。 薄膜相對於水是較為疏水性的，可從其接觸角看出。
4	模式的主要誤差來源是? 對哪些參數比較有把握?	謝謝教授的問題，在 4-3-5 節有說明。我覺得主要是有兩個誤差來源:第一個是對於接近薄膜孔徑大小分子的去除率有高估情況，第二個濃度極化現象的誤差。
5	模式如何修改?	謝謝教授的問題，已放在建議 1
6	模式與機制的關係? 模式是否有適用性?	謝謝教授的問題，由於單獨分子篩除的模式就有誤差了，所以無法繼續探討不同機制與模式的關係。

曾迪華教授

	疑問與建議	回覆
1	本研究有邏輯觀念。 實驗條件操作很複雜，該固定的要固定薄膜操作使用循環系統	謝謝教授的建議，第一部分改變操作條件時其它條件都是固定的，使用循環系統是為了使其達到穩定狀態。

2	薄膜操作實廠需要考量回收率(recovery)的影響，也應考量對通量的影響	謝謝教授的建議，已放在建議2。
3	Predict model vs rejection model，predict model 需考量通量，題目名詞可修改	謝謝教授的建議，已修改。
4	對於薄膜去除，哪種機制是主要的?	謝謝教授的問題，主要還是分子篩除是主要的，但對帶電物質則有電荷斥力的效果，吸附的效果是比較次要但還是有影響的。
5	你的實驗操作的去除率並不高，如何再提高去除率?	謝謝教授的建議，已放在建議3和4。
6	實廠(低濃度)的去除率為何?	謝謝教授的問題，依據文獻中指出的，似乎濃度不太會影響去除率，因此應該去除率是和本實驗結果是差不多的。

張怡怡教授

	疑問與建議	回覆
1	有一些名詞上的小錯誤	謝謝教授的建議，已修正。
2	討論三個機制的影響，把九個化合物全部擺出來無法凸顯機制現象，應該盡量排除其他機制的影響，再重新分組。	謝謝教授的建議，但由於有些因素導致其他機制的影響無法完全排除，因此使用全部都放的方式呈現。之後的研究可用重新分組的化合物進行。
3	對於 NF270 這個薄膜，哪一個機制佔優勢(哪一個因素相關性最強)?	謝謝教授的問題，已在 4-2-5 節有說明。

蔣本基教授

	疑問與建議	回覆
1	機制如何區分?	謝謝教授的問題，已在 3-2-3 及 4-2 做說明了。
2	做出區分機制的決策流程圖	謝謝教授的建議，已在圖 4-2-11 呈現。

Chapter 1 Introduction

1-1 Background

Emerging contaminants, such as pharmaceuticals and personal care products (PPCPs, e.g. acetaminophen and carbamazepine), endocrine disrupting compounds (EDCs, e.g. octylphenol and bisphenol A), are compounds that come from our daily lives. Due to advanced analysis instruments, low concentrations of emerging contaminants in the water environment can be detected. Consequently, they have recently caught the attention of environmentalists and the general public. Emerging contaminants can cause adverse health effect on humans and hurt aquatic microorganisms (Enick and Moore, 2007). Emerging contaminants are detected in Taiwan's rivers and hospital effluents, but their presence is unregulated by law. Conventional water treatments can only remove a few emerging contaminants; it is necessary to use advanced treatments to remove more contaminants.

Membrane processes such as nanofiltration (NF) are increasingly used in drinking water treatment to remove organic micropollutants. Several studies on the removal efficiency of PPCPs and EDCs with these high-pressure membranes have been carried out (Kimura et al., 2003a; Park et al., 2004; Yoon et al., 2006; Yangali-Quintanilla et al., 2009; Bellona et al., 2004; Nghiem et al., 2004a; Van der Bruggen et al., 2003).

Rejection mechanisms of NF membrane include size exclusion, electrostatic repulsion, and adsorption. Size exclusion is the main mechanism affecting rejection. For hydrophilic neutral solutes, rejection increases as the size of the solute increases. However, for negatively charged solutes, rejection is also governed by electrostatic repulsion. The third rejection mechanism is adsorption. Some reasearchers have studied adsorption effect recently (Comerton et al., 2007; Darling et al., 2010). Although the effect of adsorption is not as great as the other two mechanisms, it does play a role in the rejection of hydrophobic solutes. Although some researchers have studied the rejection mechanisms (Nghiem et al., 2005; Verliefde et al., 2007), the affecting parameters of each mechanism are not clear and all three mechanisms should be taken into consideration simultaneously. As a result, it is crucial to systematically understand the NF membrane rejection mechanisms and the important factors on rejection.

1-2 Objectives

The objectives of this study include the following:

1. To evaluate the effect of membrane characteristics and operating conditions on rejection.
2. To distinguish the extent of three rejection mechanisms: size exclusion, electrostatic repulsion, and adsorption.
3. To illustrate the important parameters of rejection model and discover the error patterns.

Chapter 2 Literature Review

2-1 Removal of PPCPs by nanofiltration

2-1-1 Occurrence of pharmaceutical and personal care products

Pharmaceutical and personal care products (PPCPs) including analgesics/non-steroidal anti-inflammatories, antibiotics, antiepileptics, antihypertensives, antineoplastics, antiseptics, contraceptives, sympathomimetics, lipid regulators, musks/fragrances, anti-anxiety/hypnotic agents, sun screen agents, and X-ray contrast agents are commonly used for human health. However, because of improper handling and disposal of PPCPs, trace levels of PPCPs have been observed in the aquatic environment, potentially causing harm to ecosystem and human health (Kim et al., 2007b).

Endocrine disrupting chemicals (EDCs) are substances in our environment, food, and consumer products that interfere with hormone biosynthesis, metabolism, or action resulting in a deviation from normal homeostatic control or reproduction. They include synthetic chemicals used as industrial solvents/lubricants and their byproducts (polychlorinated biphenyls, polybrominated biphenyls, dioxins), plastics [bisphenol A (BPA)], plasticizers (phthalates), pesticides [methoxychlor, chlorpyrifos, dichlorodiphenyltrichloroethane], fungicides (vinclozolin), and pharmaceutical agents

(diethylstilbestrol).

The occurrence of pharmaceutical and personal care products in the environment has been studied worldwide. PPCPs are used for human health and improvement of livestock growth and health. PPCPs including prescription and over-the-counter therapeutic drugs (e.g. antibiotics, stimulants, analgesics, and antipyretics) have been detected in the aqueous environment. The concentration of PPCPs has been detected up to several hundreds ng/L even at a μg/L level in surface water, drinking water, ground water, and reservoirs. In Taiwan, PPCPs have been detected in residential, industrial, and agricultural waste streams (Lin and Tsai 2009). It has been reported that the removal of pharmaceutical through clarification and sand filtration was not effective (Huerta-Fontela et al., 2011). Worse yet, the presence of PPCPs could result in potential risks to human health and negative environmental impacts.

Enick and Moore (2007) have reviewed the risks of pharmaceuticals in the environment. They summarized the current knowledge regarding pharmaceutical contamination of the environment and discuss specific attributes of pharmaceuticals that require special consideration. Many researchs show that PPCPs persist in water environments and can cause adverse effects on human and aquatic microorganisms.

2-1-2 Nanofiltration: good technology to remove PPCPs/EDCs

Nanofiltration has been utilized in many drinking water and wastewater treatment plants. Nanofiltration, which consumes less energy than reverse osmosis, is promising for removing dissolved organic carbon, pathogens, and viruses (Jacangelo et al., 1997). Several studies on the removal efficiency of PPCPs/EDCs with these high-pressure membranes have been carried out (Kimura et al., 2003; Bellona et al., 2004; Nghiem et al., 2004a; Van der Bruggen et al., 2003). The role of membrane filtration in water recycling schemes is steadily growing due to the high water quality that can be achieved at a moderate cost (Verliefde et al., 2007). Membrane processes employing nanofiltration (NF) are used in wastewater reclamation and in treating drinking water in order to remove micropollutants and natural organic matter (NOM). Numerous studies have shown the removal of conventional micropollutants, such as pesticides and alkyl phthalates and NOM by the NF membranes (Kiso et al., 2001).

Yangali-Quintanilla et al. (2009) suggested that chemical interactions of solutes could be ignored in a multi-component system. Rejections of ibuprofen and estrone in the bisolute control experiment were 97 and 88% (±20%), respectively. Rejections were slightly less than in a cocktail experiment (ibuprofen 99% and estrone 92%, ±20%). This implies that chemical interactions of the compounds could be disregarded.

Size exclusion, charge effect, and adsorption are major mechanisms for the

removal of impurities from water by nanofiltration. These three mechanisms can be illustrated by figure 2-1. Bellona et al. (2004) pointed out that the properties of solute, membrane, and feed solution play an important role in the permeation of solutes. Solute parameters, such as molecular weight (MW), molecular size (widith and length), hydrophilicity/hydrophobicity ($logK_{ow}$), acid association constant (pK_a), and diffusion coefficient, can be key factors affecting rejection. Membrane properties, such as molecular weight cut-off (MWCO), hydropilicity/hydrophobicity (measure as contact angle), surface charge (measured as zeta potential), pore size, and surface morphology, are major parameters controlling rejection.

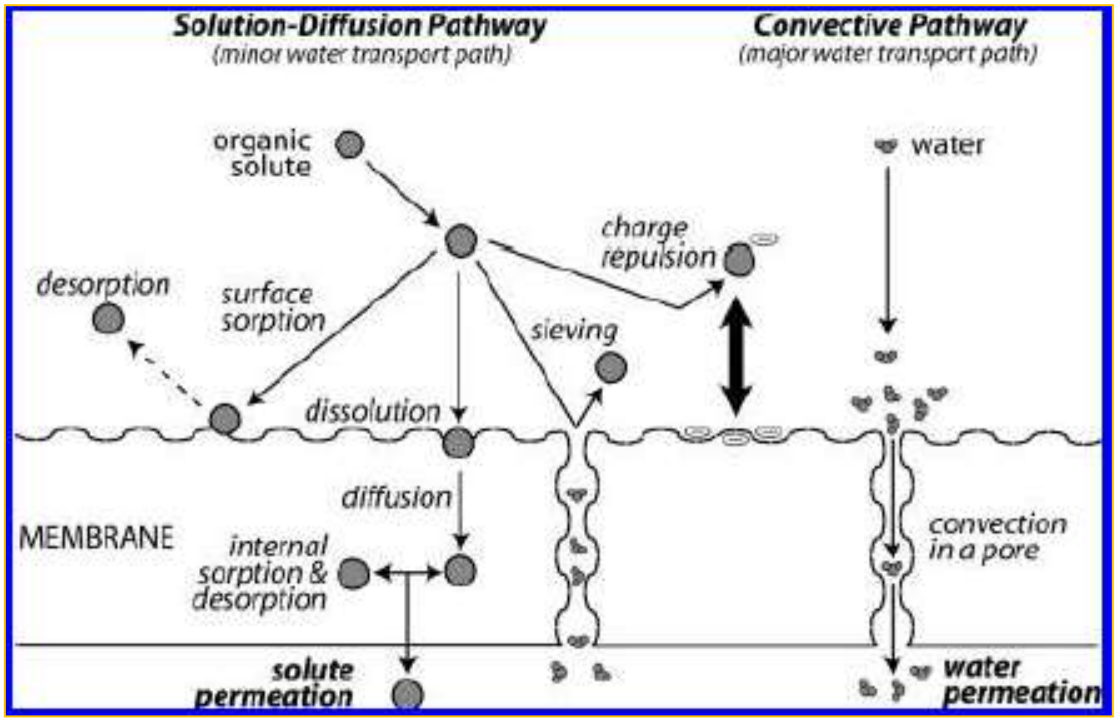

Figure 2-1 Schematic of hypothesized transport paths for water and organic microconstituents through NF membranes.
Source: Steinle-Darling et al., 2010.

2-2 Size exclusion

Size exclusion is a major mechanism in rejecting certain compounds. Yangali-Quintanilla et al. (2009) investigated the rejection of 9 PPCPs and 5 EDCs by clean and fouled NF-90 and NF-200. Rejection of hydrophilic neutral compounds had a linear relationship with molar volume and molecular length, which indicated that steric hindrance was a significant rejection mechanism for this kind of compounds.

Radjenovic et al. (2008) investigated the removal of a wide range of PPCP of 12 compounds using nanofiltration and reverse osmosis applied in a full-scale drinking water treatment plant. The highest concentration in the groundwater was recorded for carbamazepine (8.7-166.5 ng/L). Most compounds had high rejection (>85 %), except for acetaminophen (44.8-73 %), gemfibrozil (50-70 %) and mefenamic acid (30-50 %). The high rejection of uncharged solutes was brought by size exclusion (MW greater than the MWCO of nanofiltration membrane), whereas low rejection was probably due to small molecular size (MW less than the MWCO of nanofiltration membrane).

Tight membranes are mainly dominated by size exclusion, while looser membranes are decided by both size exclusion and electrostatic repulsion. For the latter, the separation efficiency of negatively charged pharmaceuticals were better as the pH value increased, and in the case of neutral pharmaceuticals, e.g. ibuprofen, adsorption

capability onto the membrane was much more significant due to the relatively high hydrophobicity (Nghiem et al., 2005).

For uncharged solutes, nanofiltration membranes are characterized by a sigmoidal rejection curve (rejection as a function of molar mass) (Van der Bruggen et al., 2002), which results in an insufficient separation between different compounds on the basis of molecular size. A typical sigmoidal rejection curve is given in Figure 2-2.

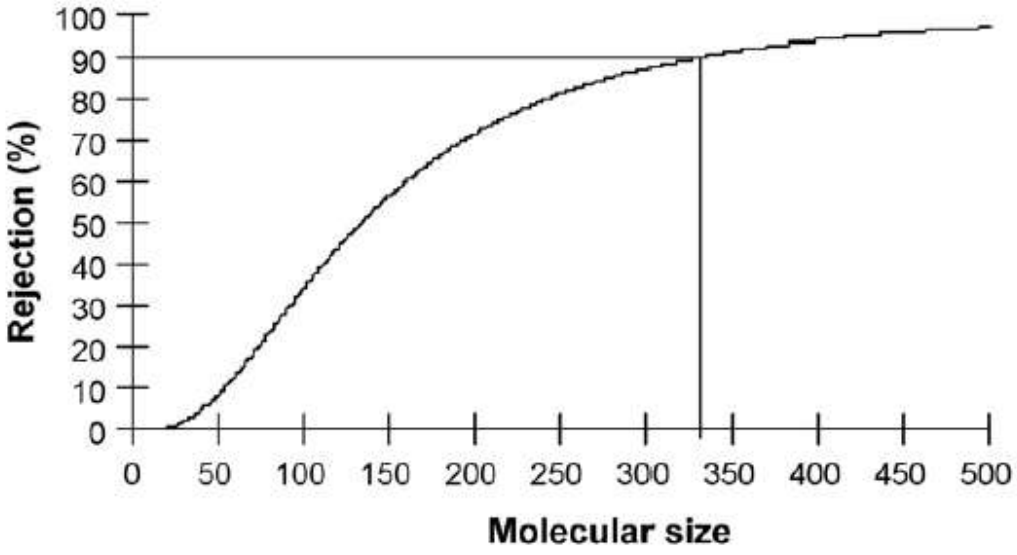

Figure 2-2 Typical sigmoidal rejection curve obtained for rejection of uncharged solutes with a nanofiltration membrane.
Source: Van der Bruggen et al., 2002.

López-Muñoz et al. (2009) determined that MWCO and pore radius of NF90 (180 Da, 0.38 nm) were lower than that of NF270 (340 Da, 0.44nm). The NF270 membrane exhibits a similar (poor) solute removal for every tested phenolic compound. The NF90 membrane, on the other hand shows different retention values for the phenolic compounds within a range from about 25% to 50%.

Kim et al. (2007a) concluded that convection is the dominant force in most cases but for more hydrophobic non-polar compounds diffusion can be more important, and convection dominance increases with membrane flux, i.e., looser membranes. Braeken et al. (2006) also mentioned that diffusion through membranes with tight pores (reflected by the MWCO) becomes more important as the molecular weight of the compound increases because steric hindrance in narrow pores mainly affects convective transport.

2-3 Electrostatic repulsion

Charge effect also determines the rejection of pharmaceuticals. As far as charge effect is concerned, electro-charge conditions of the solute and membrane can affect the mode of solute rejection. Three types of electro-charge conditions were investigated by a previous study (Radjenovic et al. 2008). Uncharged pharmaceuticals had high rejections due to the mechanism of size exclusion; negatively charged pharmaceuticals had the highest rejections because of electrostatic repulsion interaction between solutes(-) and membrane surface(-); positively charged pharmaceuticals were also rejected effectively due to a shielding effect against diffusion. Looser membranes are decided by both size exclusion and electrostatic repulsion, the separation efficiency of negatively charged pharmaceuticals were better as pH value increased (Nghiem et al., 2005).

Electrostatic repulsion is not only determined by the electro-charge of a solute but also by the nature of the membrane (Van der Bruggen et al. 1999). The influence of membrane characteristics on solute rejection is negligible when the pore size is small. When the pore size is very large, charge can be a governing factor in determining the retention of highly charged membranes.

When ion strength increases, electrostatic repulsion would decrease slightly.

Electrolytes shield molecules and membrane charges; as a result, the electrostatic repulsion becomes the main rejection mechanism for looser NF membranes (Nghiem et al., 2006).

Verliefde et al. (2007) investigated the effects of electrostatic interactions on the rejection of organic solutes with nanofiltration membranes. It was concluded that for negatively charged membranes, electrostatic repulsion leads to an increase in the rejection of negatively charged solutes and electrostatic attraction leads to a decrease in the rejection of positively charged solutes, compared to neutral solutes. Neutral and positively charged solutes engage in hydrophobic interactions with negatively charged membranes, whereas negatively charged solutes do not engage in hydrophobic interactions since they cannot approach the membrane surface. This provides proof for the theory of an increased concentration of positively charged organic solutes and a decreased concentration of negatively charged organic solutes at the membrane surface compared to the bulk fluid. This concept may be denoted as “charge concentration polarization”.

2-4 Adsorption

Comerton et al. (2007) concluded that adsorption was strongly correlated with compound $\log K_{ow}$ and membrane pure water permeability, and moderately correlated with compound water solubility. Therefore, in general, adsorption is expected to increase with decreasing compound water solubility and increasing compound hydrophobicity, as represented by $\log K_{ow}$.”

Yoon et al. (2006) investigated the removal of EDC/PPCP for 52 compounds by nanofiltration and found that rejection by nanofiltration was clearly governed by size exclusion and hydrophobic adsorption. A general separation trend due to hydrophobic adsorption as a function of octanol–water partition coefficient was observed between the hydrophobic compounds and porous hydrophobic membrane during the membrane filtration in non-equilibrium conditions.

Yangali-Quintanilla et al. (2009) studied the removals of 9 pharmaceuticals and five endocrine disrupting compounds by NF membrane filtration. Significant adsorption of hydrophobic neutral compounds to the membranes was observed; adsorption increased almost linearly in relation with log D. Adsorption of ionic and hydrophilic neutral compounds was less significant. López-Muñoz et al. (2009) mentioned that an

inverse relationship between adsorption and retention was observed. As the molecular hydrophobicity increases, the retention decreases, whereas adsorption increases.

Nghiem and Coleman (2008) reported adsorption of hydrophobic ionic compound, i.e., triclosan, on the membrane. They used 750 μg/L as the initial concentration. Adsorption capacity was about 120 μg/cm^2. For clean NF/RO membranes, no matter how hydrophilic their surfaces were, 90% triclosan were adsorbed at pH 8. Due to adsorption of hydrophobic solutes onto membranes, adsorption successfully enhances initial rejection; on the other hand, adsorption induces solute transport through the membrane via the diffusion. As a result, equilibrium rejection is lower, and this is more obvious for thin membranes. The results also show that adsorption will happen for solutes that have both the neutral and ionized form (triclosan at pH 8), but adsorption decreases significant when solutes have an almost ionized form (triclosan at pH 10).

McCallum et al. (2008) investigated adsorption and desorption of 17β-estradiol (E2) by nanofiltration membrane. They concluded that sorption processes involving E2 were found to occur predominantly at the membrane polysulfone support layer, most likely through hydrophobic interaction. Desorption of E2 to the permeate resulted in a negative apparent rejection, which occurred when the E2 concentration on the membrane was greater than the equilibrium permeate concentration.

Darling et al. (2010) investigates the relationship between trace contaminant sorption and their rejection by nanofiltration (NF) membranes. A mass balance is developed that quantitatively links the rejection decline over time seen with some adsorbing compounds to the total mass found adsorbed on the membrane. A greater tendency to sorb results in lower steady-state rejection, both when comparing compounds of similar size, as well as when comparing the same compound under different conditions. As a result, a major finding is that in the presence of competitive sorption, that is, the presence of other trace organic compounds in the membrane matrix, some compounds sorb less and are therefore rejected more than when these compounds are alone in the feed.

Nghiem et al. (2004b) investigated the rejection of four natural steroid hormones: estradiol, estrone, testosterone, and progesterones by nanofiltration (NF) membranes. At the early stages of filtration, adsorption (or partitioning) of hormones to the membrane polymer is the dominant removal mechanism. Because the adsorptive capacity of the membrane is limited, final retention stabilizes when the adsorption of hormones into the membrane polymer has reached equilibrium. At this later filtration stage, the overall hormone retention is lower than that expected based solely on the size exclusion mechanism. This behavior is attributed to partitioning and subsequent diffusion of

hormone molecules in the membrane polymeric phase, which ultimately results in a lower retention. Hormone diffusion in the membrane polymeric matrix most likely depends on the size of the hormone molecule, hydrogen bonding of hormones to membrane functional groups, and hydrophobic interactions of the hormone with the membrane polymeric matrix.

2-5 Nanofiltration predicting model

There are many models developed for predicting the performance of the nanofiltration process. The most common models for describing solute rejection include concentration polarization (film theory), the irreversible thermodynamics, solution-diffusion, and the extended Nerst-Plank model. The following discuss these above modes.

1. Irreversible thermodynamics model (Phenomenological Model)

Descriptions of solute transport in RO membranes were originally given by the irreversible thermodynamic model (Spiegler and Kedem, 1966). The membrane was treated like a black box, no membrane structural or electrical parameters were acquired and scarce information about the transport mechanisms inside the membrane could be obtained

The non-equilibrium thermodynamic transport equation is composed of two driving forces, convection and diffusion (Kedem and Katchalsky, 1958; Yoon et al., 2005):

$$J_s = \text{diffusion} + \text{convection} = \omega\Delta\Pi + (1-\sigma)\, C_{avg}\, J_v \qquad (2\text{-}1)$$

where J_s is the solute flux (mol/m^2s) occurring due to diffusion and convection, ω is the

molecular transport coefficient (solute permeability) (mol/m^2sPa), $\Delta\Pi$ is the osmotic pressure gradient (Pa), σ is the molecular reflection coefficient (dimensionless), C_{avg} is the bulk-fluid interfacial concentration between feed and permeate side (mol/m^3), and J_v is the solvent flux (m^3/m^2s).

For pressure-driven membrane process, the solute flux through the membrane can be described as the sum of a convective flux and a diffusive flux. This model is derived from the aspect of thermodynamics (i.e. free energy, entropy) to deal with membrane separation, not considering membrane structure and transport. As a result, the membrane is regarded as a black box. The following Spiegler-Kedem equation is the most widely used in the field (Spiegler and Kedem 1966), which assumes that reflection coefficient (σ) and hydraulic permeability ($P_)$ are constants with respect to salt concentration.

$$R_r=\frac{\sigma[(1-\exp(-Pe)]}{1-\sigma\exp(-Pe)}=1-\frac{1-\sigma}{1-\sigma\ \exp(-pe)} \quad (2\text{-}2)$$

$$Pe=\left(\frac{1-\sigma}{P_s}\right)J_v \quad (2\text{-}3)$$

where P is the solute permeability and σ is the reflection coefficient.

2. Concentration polarization model (Film theory model)

In a membrane filtration process, the solute is rejected by the membrane so the concentration near the membrane surface increases. This build-up in solute concentration at the membrane-liquid interface is called concentration polarization. At steady-state, the solute flux is constant throughout the membrane. The equation for concentration polarazation is described as below:

$$J_v C - \left(D \frac{dc}{dx} \right) = J_v C_p \tag{2-4}$$

The boundary conditions are:

$$C = C_m \text{ at } X = 0 \tag{2-5}$$

$$C = C_p \text{ at } X = \delta \tag{2-6}$$

Integrate Eq. (2-3) and rearrange the equation, one has the following expression: (Murthy and Gupta 1997).

$$\frac{R}{1-R} = \frac{R_r}{1-R_r} \times \exp\left(-\frac{J_v}{k} \right) \tag{2-7}$$

$$R = \frac{C_b - C_p}{C_b} \tag{2-8}$$

$$R_r = \frac{C_m - C_b}{C_b} \tag{2-9}$$

where J_v is the pure water solvent flux, k is the mass transfer coefficient, C_p and C_b are permeate and bulk concentration, respectively, and C_m is the concentration at the membrane surface.

Murthy and Gupta (1997) combined the Spiegler-Kedem equation and film theory to derive a new working equation. By supplying the observed rejection data and solvent flux data, taken at different pressures but at a constant feed rate and constant feed concentration for each set, the mass transfer coefficient, k, can be estimated numerically.

3. Extended Nerst-Planck model (Hydrodynamic Model)

The extended Nerst-Planck model considers all driving forces, namely physical convection, chemical diffusion, and electrical interactions, to determine the solute flux through a membrane (Bowen et al., 1997; Garba et al., 2000). The equation for determining the solute flux is described as follows:

$$j_i = -D_{i,p}\frac{dc}{dx} - \frac{z_i c_i D_{i,p}}{RT} F \frac{d\psi_m}{dx} + K_{i,c} c_i V \qquad (2\text{-}10)$$

where the first term on the right hand side describes the effect of concentration gradient caused by diffusion; the second term describes the effect caused by electric potential gradient and electrostatic force; and the third term describes the effect caused by convection. If the solute is uncharged, the second term can be neglected. $D_{i,p}$ is hindered diffusivity, z_i is the valent of the ion, F is the Faraday's constant, ψ_m is the electric potential in the membrane (axis direction), $K_{i,c}$ is the hinderance factor for convection.

From the equation, we can derive the rejection for uncharged solutes (Verliefde et.

al., 2009):

$$R = 1 - \frac{\beta\varphi K_c}{1-\left((1-\varphi K_c)\, exp(-Pe)\right)} \quad (2\text{-}11)$$

$$\mathrm{Pe} = \frac{\mathrm{JvKc\Delta x}}{\mathrm{KdD\varepsilon}} \quad (2\text{-}12)$$

R: uncharged solute rejection, β: hydrodynamic concentration polarization, φ: partition coefficient, *K*c or *K*d: steric hindrance coefficients against convective transport or diffusive transport, Jv: solvent fluxes, D: solute diffusion coefficient, Δ*x*/ε: ratio of membrane thickness to membrane porosity.

And the rejection for charged solutes (Verliefde et. al., 2009):

$$\mathrm{R} = 1 - \frac{\beta_{\mathrm{charge}}\beta\varphi\mathrm{K_c}}{1-\left((1-\varphi\mathrm{K_c})\exp(-\mathrm{Pe})\right)} \quad (2\text{-}13)$$

$$\beta_{\mathrm{charge}} = \exp(-Z_m\, \Psi F/RT) \quad (2\text{-}14)$$

β_{charge} is charge concentration polarization.

*Z*m is the organic ion valence, Ψ is the membrane potential (in mV), *F* is Faraday's constant, *R* is the universal gas constant, *T* is the temperature (in K).

Chapter 3 Materials and Methods

3-1 Research flowchart

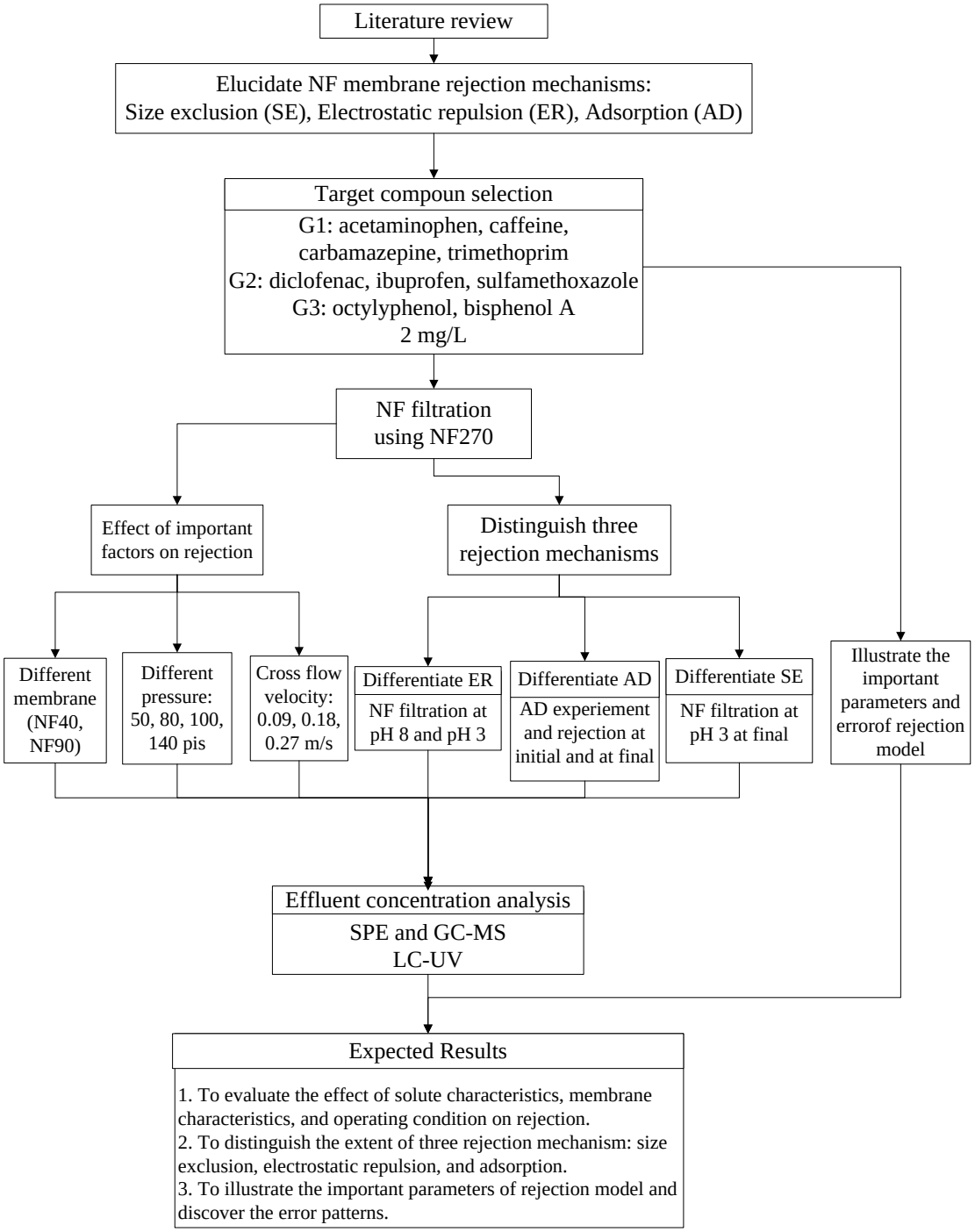

Figure 3-1 Research flowchart

3-2 Experimental design

3-2-1 PPCPs/EDCs target compounds selection and classification

The main affecting parameters of size exclusion (SE) are target compound size and membrane pore size. Target compound size can be represented by use molar weight (MW), and membrane pore size can be represented by molar weight cut-off (MWCO). When target compound's MW > membrane MWCO, its rejection will be higher. The main affecting parameters of electrostatic repulsion (ER) are target compound and membrane charge, both will be affected by pH. Membrane charge can be represented by zeta potential, target compound charge is related to its pKa value. When the target compound's pKa < pH, it will have negative charge. The main affecting parameters of adsorption (AD) are target compound and membrane hydrophobicity. Membrane hydrophobicity can be represented by contact angle, and the target compound charge is related to its log Kow or log D value. Log D is a parameter used to calibrate log Kow target compound's charge effect, using pH and pKa to calibrate. When target compound's log Kow or log D >3, it can be considered hydrophobic. Otherwise, it is hydrophilic.

Nine target compounds were classified into three groups according to characteristics of compounds and speculated rejection mechanisms. Because size

exclusion effect occurs for all compounds, therefore, size effect was not considered for classification purpose. The target compounds were classified into three groups (Table 1): Solutes with $pK_{a1} > 8$ (netural charge at pH 8) and log $K_{ow} < 3$ form group 1 (G1); Solutes with $pK_{a1} < 8$ (negative charge at pH 8) form group 2 (G2); Solutes with $pK_{a1} > 8$ (netural charge at pH 8) and log $K_{ow} > 3$ form group 3 (G3). Governing rejection mechanisms for the three groups of compounds are size exclusion (SE) for G1, electrostatic replusion (ER) and size exclusion (SE) for G2, and adsorption (AD) and size exclusion (SE) for G3. Those nine target compounds were selected for this study due to their frequent existence in the aquatic environment with compound characteristics suitable for this study.

Table 3-1 Classification of target compounds and their physico-chemical properties

Classification		Target Compound	MW	$logK_{ow}$	pK_a	Analysis
G1	$pK_{a1} < 8$ (neutral), log $K_{ow} < 3$	Acetaminophen	151	0.46	9.5	GC-MS
		Caffeine	194	0.07	14	GC-MS
		Carbamazepine	236	2.5	13.9	GC-MS
		Trimethoprim	290	0.9	17.3, 7.1	LC-UV
G2	$pK_{a1} < 8$ (-) charge	Ibuprofen	206	3.97	4.4	LC-UV
		Sulfamethoxazole	253	0.89	5.6	LC-UV
		Diclofenac	296	4.51	4.08	GC-MS
G3	$pK_{a1} < 8$ (neutral), log $K_{ow} > 3$	Octylphenol	206	5.28	10.3	GC-MS
		Bisphenol A	228	3.3	10.3	LC-UV

3-2-2 Nanofiltration membrane characteristic

A nanofiltration membrane NF-270 was mostly used for this study. The membrane NF40 was also used due to its greater thickness, and the membrane NF90 was used as well due to its smaller pore size. Their properties are listed in Table 3-2.

Table 3-2 Properties of nanofiltration membrane used in this study (Dow Filmtec)

Membrane	NF270	NF90	NF40
Manufacturer	Dow Filmtec	Dow Filmtec	Dow Filmtec
Membrane Material	Polyamide composited	Polyamide composited	Polyamide composited
Backing Material	Polyester	Polyester	Polyester
MWCO	200-400	200	200-400
Water Permeability	13.5 (L/m^2 h/bar)	11.3 (L/m^2 h/bar)	
Charged	"-" (neutral pH)	"-" (neutral pH)	"-" (neutral pH)
Thickness	0.2 (mm)		0.76(mm)
Pore radius	0.44 (nm)	0.38(mm)	0.44 (nm)
pH range	2~11	2~11	2~11
Feed temperature range	4~40 ℃	4~35 ℃	4~40 ℃
NaCl rejection	40~60	85~95	40~60
$MgSO_4$ rejection	>95	>96	95
contact angle	29~32		

3-2-3 Distinguishing three rejection mechanisms

The filtration process was operated at pH 8 for observing all three rejection mechanisms including size exclusion, electrostatic repulsion and adsorption. The filtration process was operated at pH 3 for observing the change in rejection mechanisms due to the minimization of an electrostatic repulsion mechanism. At pH 3, the pKa of each target compound is greater than pH 3 and the surface charges of the compounds are in a neutral state (no negative charge). Third, the adsorption effect can be observed by the change in feed concentration, assuming the feed concentration decrease is caused by adsorption on membrane. The adsorption capacity can also be evaluated by the adsorption experiment.

The effect of electrostatic repulsion can be evaluated by knowing the difference in rejection at pH 8 and pH 3. The effect of adsorption can be evaluated by subtracting the rejection at initial and the rejection at final stage. The effect of size exclusion can be determined by the difference in rejection at pH 3 at the final stage.

3-2-4 Influence of operating condition on nanofiltration rejection

To illustrate the extent of pertinent factors affecting rejection, five compounds were selected for further study. They include compounds of different sizes forming group 1 (acetaminophen, caffeine, carbamazepine), one group 2 compound (diclofenac), and one group 3 compound (octylphenol).

To elucidate the size exclusion effect, a nanofiltration experiment is carried out at different transmembrane pressures (50, 80, 100, 140 psi) at cross flow velocity of 0.18m/s. The experiment is also carried out at different cross flow velocities (0.09, 0.18, 0.27 m/s) at transmembrane pressure of 100 psi.

3-2-5 Feed concentration, mixed solute and calculation of rejection

To enhance solubility, stock solutions of concentration 1000 mg/L with methanol as the solvent were used. Solutions were then diluted to an initial concentration of 2 mg/L in 5 L water, with 20 mM NaCl and 1mM HCO_3.

In this research, mixed solutes were used to conduct the nanofiltration experiments. To investigate whether mixed solutes will have an effect on rejection, the rejection of a single solute by a nanofiltration membrane was conducted. Fig 3-2 shows the results of rejections of single and mixed solutes by the NF270 membrane at pH 3 and pH 8. Although the rejections of single and mixed solutes show some difference, the

difference is smaller than 5% and can be due to experimental error, so the difference is insignificant. Since the use of mixed solutes for experiments is more convenient, mixed solutes are used in the experiments.

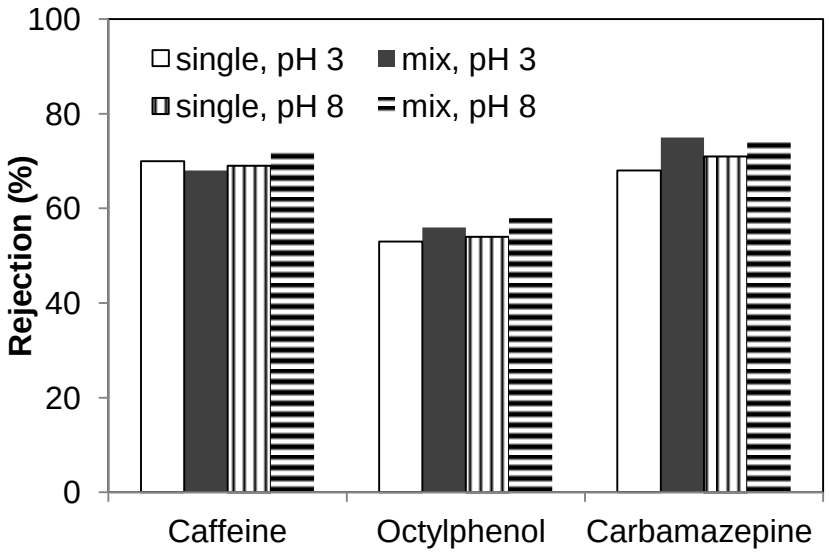

Figure 3-2 Compared rejections of single and mixed solutes at pH 3 and pH 8

The rejection is calculated based on the feed concentration (C_f): R= 1- C_p / C_f, not based on the initial concentration (C_i): R= 1- C_p / C_i. Calculating rejection based on the initial concentration is not accurate because the solute will be adsorbed on the membrane, causing the feed concentration to decrease.

3-3 NF membrane Filtration process

A cross-flow module was used for the filtration test. Figure 3-3 shows a schematic diagram of the filtration module used in this study. The surface area of the membrane was 140 cm^2 (14.6 cm×9.5 cm) and the cross-sectional area was 1.9 cm^2 (9.5 cm×0.2 cm). The membranes were stored in 1.5% (w/w) sodium persulfate ($Na_2S_2O_8$) to avoid oxidation and being dried (Dow Filmtec). The membrane taken from the stored solution must be rinsed with DI water.

Filtration protocol includes two phases: compaction and filtration. After filtration, DI water is used to clean the experimental equipment.

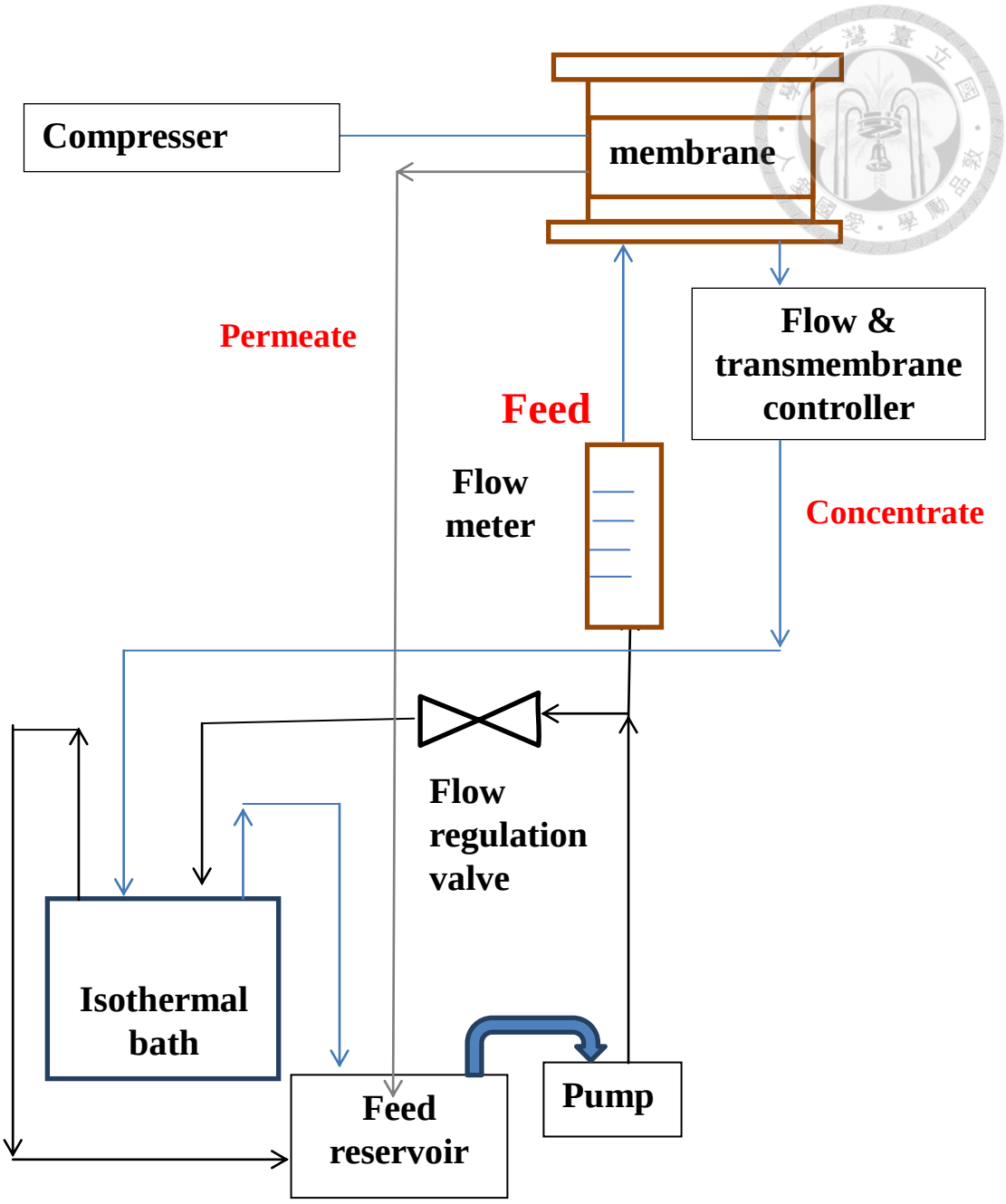

Figure 3-3 Schematic diagram of the filtration module

Phase I compaction: Before the filtration test, the membrane must be rinsed with DI water and filtrated with DI water for at least 4 hours to reach the steady-state solvent flux, and operated at 100 psi pressure to avoid membrane pore size change.

Phase 2 Filtration: Add the target compound solution, use 20 mM NaCl to control

ionic strength, use 5 mM NaHCO3 as a buffer, and then use HCl or NaOH to adjust pH to 8 or 3. The total volume of feed water is about 5 L. Before doing the experiments, stir the feed tank until it is uniform. Experiments operate at a constant temperature (22 ^{o}C).

3-4 Membrane adsorption test process

Adsorption tests start by taking the membrane from the preservation solution, rinsing it with DI water, cutting it into small species, and putting into the container. Set the initial concentration of the feed solution and add the membrane into the feed. Then, measure the concentration along with time, in order to know the adsorption limit of membrane for each target compound. Jar test equipment (shown in Figure 3-4) with 100 rpm was used to balance the solution in the feed. During the period of the experiment take a sample every day.

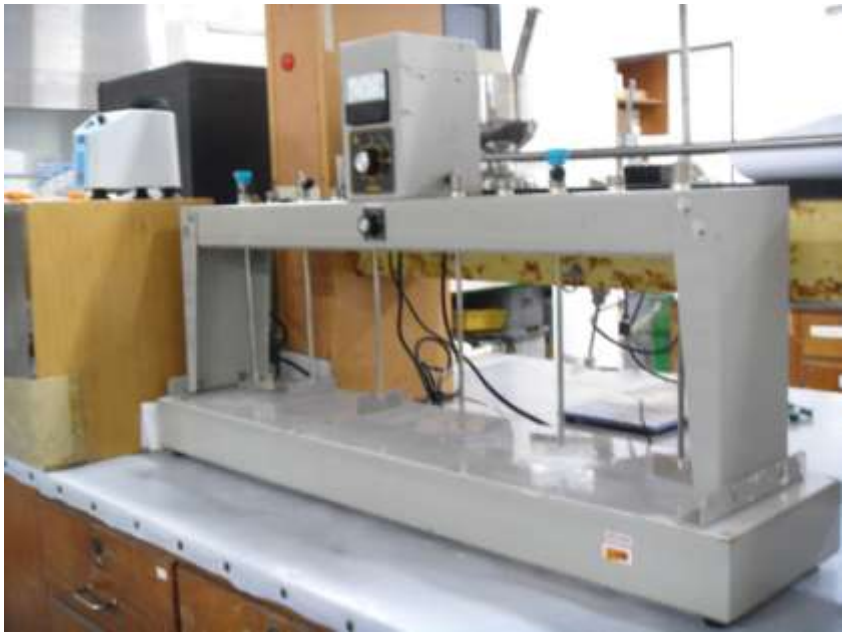

Figure 3-4 Photo of Jar test equipment

3-5 Analytic methods

3-5-1 Solid Phase Extraction (SPE)

For each sample, an Oasis HLB cartridge (60 mg, 3 mL) was conditioned with ethyl acetate, methanol & DI water (each 2 × 2 mL). The water samples (1~10 mL) were then passed through the cartridge. On completion of the extraction, the cartridges were eluted with 1 mL of a 50:50 mixture of ethyl acetate: methanol.

3-5-2 GC-MS analysis

The photo of GC-MS is shown in Figure 3-5. The concentrations of solutes were determined by an Agilent 7890A gas chromatography equipped with Agilent 5975C VL

MSD with Triple-Axis Detector in selected ion monitoring mode. An Agilent 19091s-433 column (30 m×0.25 mm i.d, film thickness 0.25 μm) was used for chromatographic separation. The carrier gas was helium at a constant flow rate of 1.0 mL/min. A splitless injection technique was used to inject 1 μL of sample at an injection port temperature of 280 ◦C. For the analysis of all compounds, the oven program was as follows: 100 ◦C for 1 min and then raise to 275 ◦C at a rate of 10 ◦C/min; total analysis time is 18.5 min. Postrun is at 320 ◦C for 2 min. The detector was used predominantly in selected ion mode (SIM). The electron impact source temperature was 230 ◦C with an electron energy of 70 eV. The quadruple temperature was 150 ◦C, the GC interface temperature was 280 ◦C, and the injector's temperature was 300 ◦C. The instrument was tuned on perfluorotributylamine. A scan range of 50–500*m*/*z* was used for a full scan analysis of selected samples. Table 3-3 shows the GC-MS analytical parameters in this research.

Figure 3-5 Photo of Jar test equipment

Table 3-3 GC-MS analytical parameters

Target compound	Abbreviation	Retention time (min)	Mass faction
Octylphenol	OP	8.7	109, 151
acetaminphen	ACM	10.4	135, 206
Caffeine	CAF	11.4	109, 194
Carbamazepine	CBM	12.8	165, 193
Diclofenac	DCF	14.5	242, 277

3-5-3 LC-UV analysis

An Agilent 1200 series (Agilent, Palo Alto, CA, USA) equipped with a Varian Polaris C18-A column (with diameter, length and pore size of 4.6 mm, 250 mm and 5 μm, respectively) and an ultraviolet (UV) detector was used for the analysis of the PPCPs. Figure 3-6 shows a photo of the HPLC instrument. HPLC grade methanol and 20 mM KH_2PO_4 buffer solution, in which pH was adjusted to 3.0 using NaOH and/or

HCl, were used as the mobile phase. The mobile phase was delivered at 0.8 mL/min through the column. The HPLC gradient program is shown in table 3-4.

The sample injection volume was 10 μL. Column temperature was controlled at 30℃. All target compounds were eluted out of the column within 12 minutes. Calibration curves with coefficients of determination (R^2) greater than 0.995 were used. Table 3-5 shows the HPLC/UV analytical parameters in this research.

Figure 3-6 Photo of the HPLC instrument

Table 3-4 HPLC mobile phase gradient condition

	pH 3 buffer(%)	methanol(%)
0	80	20
2	80	20
6	20	80
8	20	80
12	80	20
15	80	20

*Buffer is 20 mM phosphate.

Table 3-5 HPLC analytical parameters

Target compound	Abbreviation	Retention time (min)	Wavelength detected (nm)
acetaminphen	ACM	8.45	230
trimethoprim	TMP	9.07	230
sulfamethoxazole	SMX	9.65	275
bisphenol A	BPA	10.9	275

3-6 NF membrane rejection model

3-6-1 Irreversible thermodynamics model

The real retention is determined using the Spiegler-Kedem equation:

$$R_r = 1 - \frac{C_p}{C_m}$$

$$= 1 - \frac{1-\sigma}{1-\sigma\ \exp(-pe)} \qquad (3-1)$$

$$pe = \left(\frac{1-\sigma}{P_s}\right) J_v \qquad (3-2)$$

where c_p is the solute concentration in the permeate solution; c_m is the solute concentration on the membrane surface; σ is the reflection coefficient; P is the solute permeability; J_v is the water flux (m/s).

The concentration polarization is classically derived by making a mass balance across the concentration polarization layer. Note that the real rejection R_r is not the same as the observed rejection R because of concentration polarization. The film theory model shows that R is related to R_r via the following equation (Murthy and Gupta, 1997):

$$\frac{1-R_r}{R_r} = \frac{1-R}{R} \times \exp\left(-\frac{J_v}{k}\right) \qquad (3\text{-}3)$$

Substituting Eq. (3-1) into Eq. (3-2) and rearranging results in the following equation:

$$R = 1 - \frac{\beta * (1-\sigma)}{\sigma[1-\exp(-pe)] + \beta * (1-\sigma)} \qquad (3-4)$$

The reflection coefficient (σ) and solute permeability (P) can be predicted from

transport models, i.e., the SHP and TMS models. Pe is peclet number.

3-6-2 Extended Nerst-Planck model

The well-known Spiegler–Kedem equation for steady-state transport in pressure-driven membrane processes is:

$$J_s = \frac{J_v}{\varepsilon} C_p = -K_d D_\infty \frac{dc}{dx} + \frac{J_v}{\varepsilon} \mathrm{K_c} c \tag{3-5}$$

Boundary conditions

at $x = 0$ (within the membrane at the feed side):

$$\mathrm{c}\ (\mathrm{x} = 0) = c_f = \varphi C_m = \varphi \beta C_f \tag{3-6}$$

at $x = \Delta x$ (within the membrane at the permeate side):

$$\mathrm{c}(\mathrm{x} = \Delta \mathrm{x}) = c_{fp} = \varphi C_p \tag{3-7}$$

$$\text{and knowing } \varphi = \frac{c_p}{C_p} = \frac{c_f}{C_m} = \frac{c_f}{\beta C_f} \tag{3-8}$$

Using the extended Nernst-Planck Model + concentration polarization model (Verliefde et. al., 2009), rejection of uncharged solute can be represent by equation:

$$\mathrm{R} = 1 - \frac{\beta \varphi \mathrm{K_c}}{1 - \left((1 - \varphi \mathrm{K_c}) \exp(-\mathrm{Pe})\right) - \varphi \mathrm{K_c}((1-\beta)} \tag{3-9}$$

$$\mathrm{Pe} = \frac{\mathrm{JvKc}\Delta \mathrm{x}}{\mathrm{KdD}\varepsilon} \tag{3-10}$$

R: uncharged solute rejection, β: hydrodynamic concentration polarization, φ: partition coefficient, *K*c or *K*d: steric hindrance coefficients against convective transport or diffusive transport, Jv: solvent fluxes, D: solute diffusion coefficient, Δ*x*/ε: ratio of

membrane thickness to membrane porosity.

For charged solutes:

$$R = 1 - \frac{\beta_{charge}\beta\varphi K_c}{1-((1-\varphi K_c)\exp(-Pe))-\varphi K_c((1-\beta)} \quad (3\text{-}11)$$

$$\beta_{charge} = \exp(-Z_m \Psi F/RT) \quad (3\text{-}12)$$

β_{charge} is charge concentration polarization. *Z*m is the organic ion valence, Ψ is the membrane potential (in mV), *F* is Faraday's constant, *R* is the universal gas constant, *T* is the temperature (in K).

3-6-3 Determination of common model parameters

3-6-3-1 Equipment parameters

The equipment used was a flat nanofiltration module. The parameters of the module are flow (Q) channel height (h), channel length (l), channel width (w), surface area [A_s = l*w], cross-sectional area [A_c = w*h], and hydraulic diameter [d_h = 2*wh/(w+h)]. Temperature was set at constant value of 22 ◦ C, and water density and viscosity are constant as well. Membrane radius is provided by the manufacturer. Transmembrane pressure ΔP, feed flow rate Q_f, and permeate flow rate Q_p can be measured during the experiment. The cross flow velocity is determined as [$v = Q_f/A_c$] and solvent flux as: [$J_v = Q_p/A_s$].

3-6-3-2 Diffusion coefficient

The diffusion coefficient of the compound in water (D_s) is calculated from the Hayduk and Laudie method and shown below:

$$D_s = \frac{13.26\times10^{-5}}{\mu^{1.14}V_a^{0.589}} \left(\frac{cm^2}{s}\right) \quad (3\text{-}13)$$

where μ: viscosity of water (cP);

V_a is molar volume = MW/ρ = molecular weight/ density (cm^3/g)

3-6-3-3 Mass transfer coefficient

The mass-transfer coefficient k, which is a function of feed flow rate, cell geometry and solute system, can be calculated for laminar flow using the Deissler equation：

$$Sh = 0.065\ Re^{0.875} * Sc^{0.25} \quad (3\text{-}14)$$

where Sherwood number：$Sh = \frac{kd_h}{D_s}$ (3-15)

Reynolds number：$Re = \frac{\rho d_h v}{\mu}$ (3-16)

Schmidt number：$Sc = \frac{\mu}{D_s \rho}$ (3-17)

Substitution of Eq. (4-4) to (4-6) into Eq. (4-3) enables the k value to be determined.

3-6-3-4 Hydrodynamic concentration polarization factor

The hydrodynamic concentration polarization is defined by film theory as follows:

$$\beta = \frac{C_m - C_p}{C_f - C_p} \approx \frac{C_m}{C_f} = \exp\left(\frac{J_v}{k}\right) \quad (3\text{-}18)$$

where β is the hydrodynamic concentration polarization factor, C_m, C_f and C_p are the solute concentrations at the membrane surface, in the bulk of the feed and in the permeate, respectively, and k is the mass transfer coefficient.

3-6-3-5 Ratio of membrane thickness to porosity (Δx/ ε)

The Hagen-Poiseuille relationship between the pore radius and the thickness-porosity is as follows:

$$\frac{\textbf{membrane thickness}}{\textbf{membrane porosity}} = \left(\frac{\Delta x}{\varepsilon}\right) = \frac{r_p^2\,\Delta P}{8\mu\, J_v} \qquad (3\text{-}18)$$

where μ: represents the dynamic viscosity of the solution(kg/ms); r_p is pore radius and $\Delta x/A_k$ is the thickness-porosity ratio; ΔP: transmembrane pressure.

3-6-4 Obtain Irreversible thermodynamics model parameter

3-6-4-1 Solute radius

In this model, hydrodynamic radius, which considers solvent bound to solute, is used to represent solute radius:

$$r_s = \left(\frac{3 * 10^{-6}\, Va}{4\pi No}\right)^{1/3} \qquad (3-20)$$

Ratio of solute to pore radius: $\lambda = r_s / r_p$

3-6-4-2 Parameters of SHP model

The SHP model is used for describing the mechanism of size exclusion, and it can be simplified by the following equations:

$$\sigma = 1 - \left(1 + \frac{16}{9}\lambda^2\right)(1-\lambda)^2[2-(1-\lambda)^2] \qquad (3-21)$$

$$P = D_s(1-\lambda)^2\frac{\varepsilon}{\Delta x} \qquad (3-22)$$

where P is the solute permeability. Reflection coefficient σ is the limiting value of rejection when filtration flow overtakes diffusion, which is when flux is very large.

3-6-5 Obtain extended Nerst-Planck model parameter

3-6-5-1 Solute radius

The Stokes radius will be used as an approximation for the solute radius in this model:

$$r_s = \left(\frac{k_b T}{6\pi\mu D_s}\right) \qquad (3-23)$$

k_b is Boltzmann constant = $1.38*10^{-23}$ J/K.

Ratio of solute to pore radius: $\lambda = r_s / r_p$

3-6-5-2 Hindrance factors

There are several methods for calculating the hindrance factors. The method of Bowen et al. (1997) is mostly used. In this study, the method shown below was used:

$$\varphi = (1-\lambda)^2 \qquad (3-24)$$

$$K_c = (2-\varphi)(1+0.054\lambda-0.988\lambda^2+0.441\lambda^3) \qquad (3-25)$$

$$K_d = 1-2.3\lambda+1.154\lambda^2+0.224\lambda^3 \qquad (3-26)$$

φ is partition coefficient.

K_c & K_d: steric hindrance coefficients against convective transport and diffusive transport, respectively.

3-6-6 Model sensitivity test

Several model parameters are changed, including transmembrane pressure, cross flow velocity and membrane pore radius. The experimental and predicted result tendencies were compared.

Chapter 4 Results and Discussion

4-1 Effect of membrane characteristics and operating conditions

4-1-1 Effect of membrane thickness and pore radius on rejection

In this research, NF270 was mainly used to conduct the filtration experiments. Two other membranes are selected to be compared with the rejection by the NF270 membrane. The NF40 membrane has the same pore radius as NF270, but it is thicker than NF270. NF90 membrane has the same thickness as NF270, but its pore radius is smaller than NF270.

Permeate flow rates and solvent fluxes of NF270, NF40, and NF90 membrane are shown in Figure 4-1-1. The solvent flux is permeate flow rate divided by the surface area of the nanofiltration membrane. NF270 has a larger solvent flux than NF40 and NF90. This is because when the membrane is thicker or the pore radius is smaller, it is more difficult for solvents and solutes to penetrate the membrane, thus resulting in a lower solvent flux.

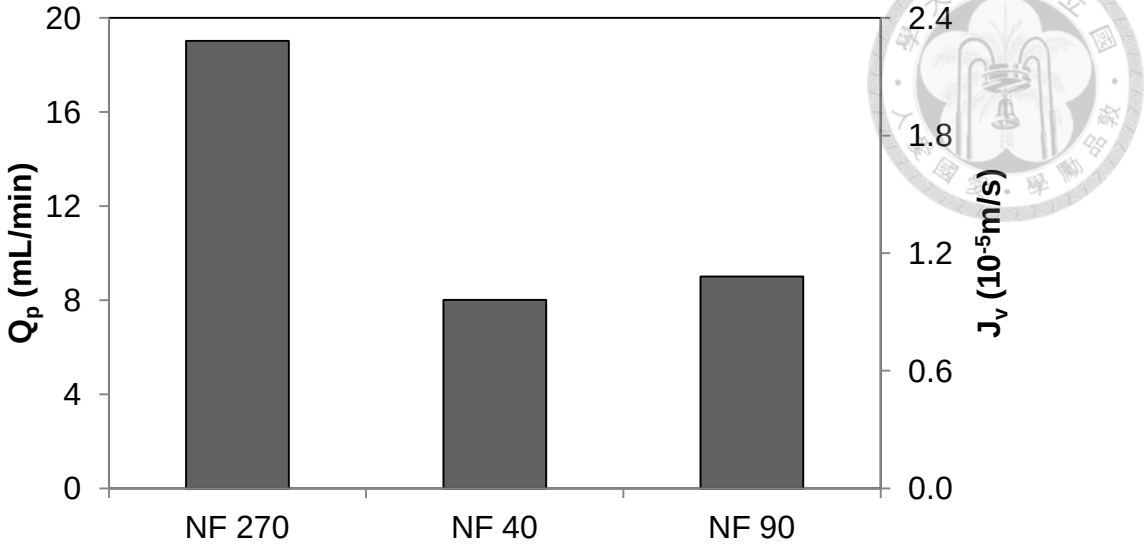

Figure 4-1-1 Permeate flow rate and solvent flux for various types of nanofiltration membrane at transmembrane pressure 100 psi, pH 3, and cross flow velocity 0.27 m/s.

The comparison between the rejection of mixed solutes by NF270 and NF40 membranes at pH 3 is shown in Figure 4-1-2. NF40 has slightly higher rejection than the NF270 membrane. The rejections of acetaminophen, caffeine, carbamazepine, diclofenac, and octylphenolare by NF40 membrane are 59%, 79%, 86%, 68%, and 71%, respectively. The NF40 rejection is higher because this membrane is thicker than NF270, thus hindering solute transport.

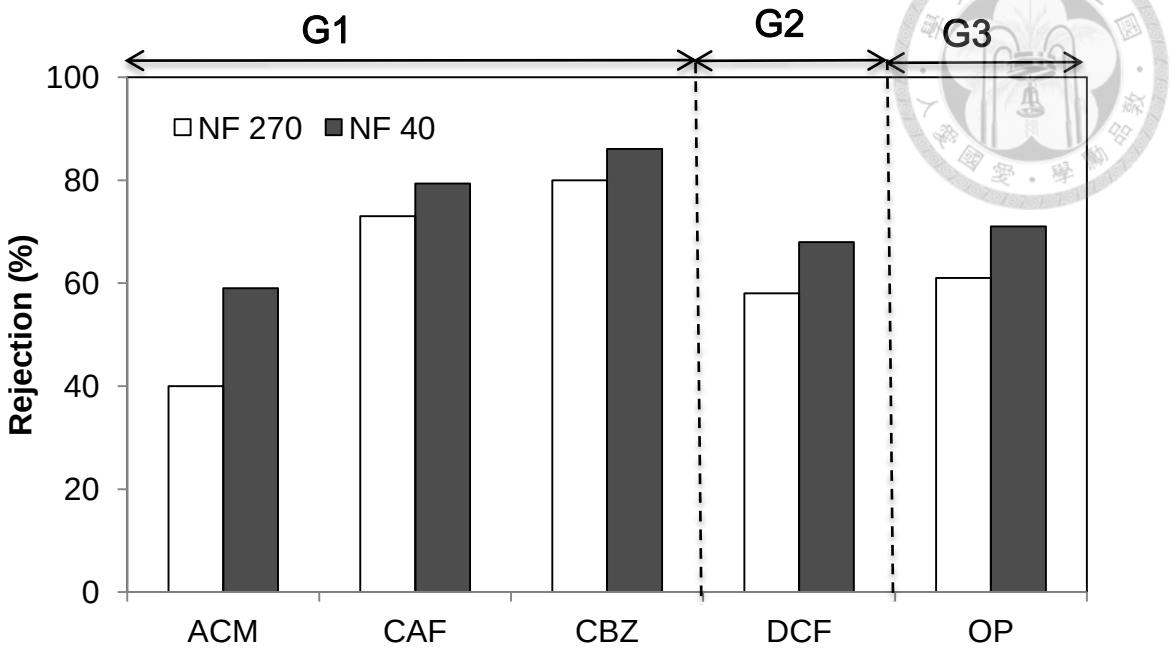

Figure 4-1-2 Rejections of selected solutes by NF-270 and NF40 membrane at pH 3, transmembrane pressure of 100 psi, and cross flow velocity of 0.27 m/s.

The comparison between the rejections of mixed solutes by NF270 and NF90 membrane at pH 3 is also shown in Figure 4-1-3. The overall trend indicates that the NF90 membrane has a very good rejection, exceeding 86% for all compounds. For small compounds like acetaminophen, when the membrane pore radius decreases, rejection significantly increases. Rejections of octylphenol and diclofenac are slightly lower than those of other compounds, and this is likely due to adsorption on the nanofiltration membrane.

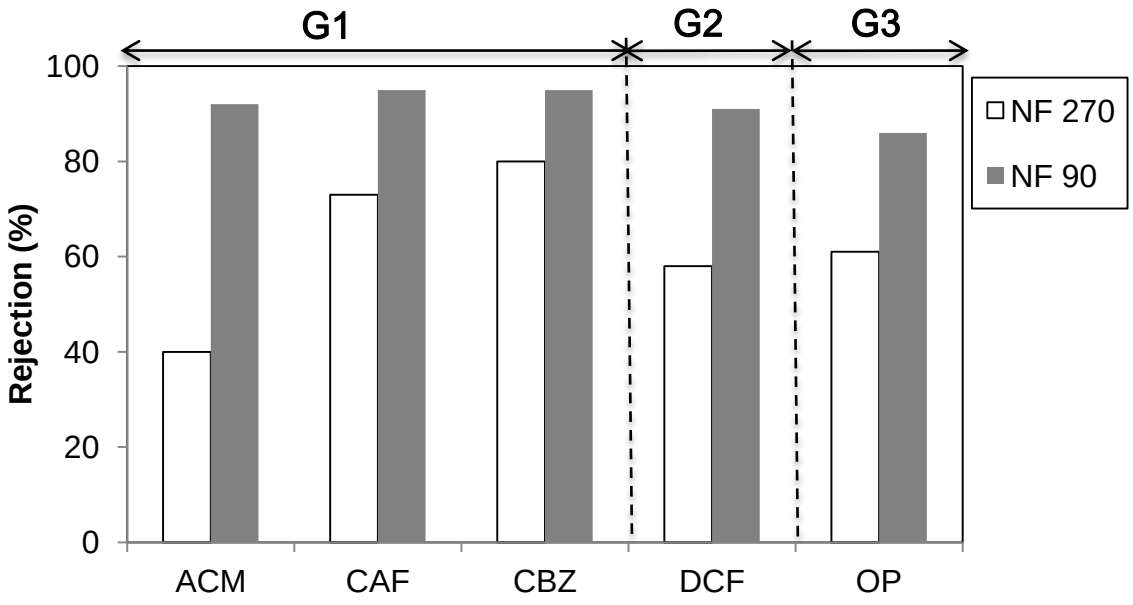

Figure 4-1-3 Rejections of selected solutes by NF-270 and NF40 membranes at pH 3, transmembrane pressure of 100 psi, and cross flow velocity of 0.27 m/s.

To compromise the solvent flux and rejection results associated with selected NF membranes, i.e., NF270, NF90, NF40, the NF270 was selected for further study.

4-1-2 Effect of transmembrane pressure on flux and rejection

The operating condition may affect rejection, e.g., transmembrane pressure and cross flow velocity are important parameters. In the following section, these effects are considered.

Figure 4-1-4 shows the NF-270 membrane solvent flux versus transmembrane pressure at pH 3. It shows that NF270 membrane peameate flux increases linearly as transmembrane pressure increases. The solvent flux increases from $1.33*10^{-5}$ m/s at transmembrane pressure 50 psi to $4.16*10^{-5}$ m/s at transmembrane pressure 140 psi. At the same transmembrane pressure, changing cross flow velocity does not vary the solvent flux.

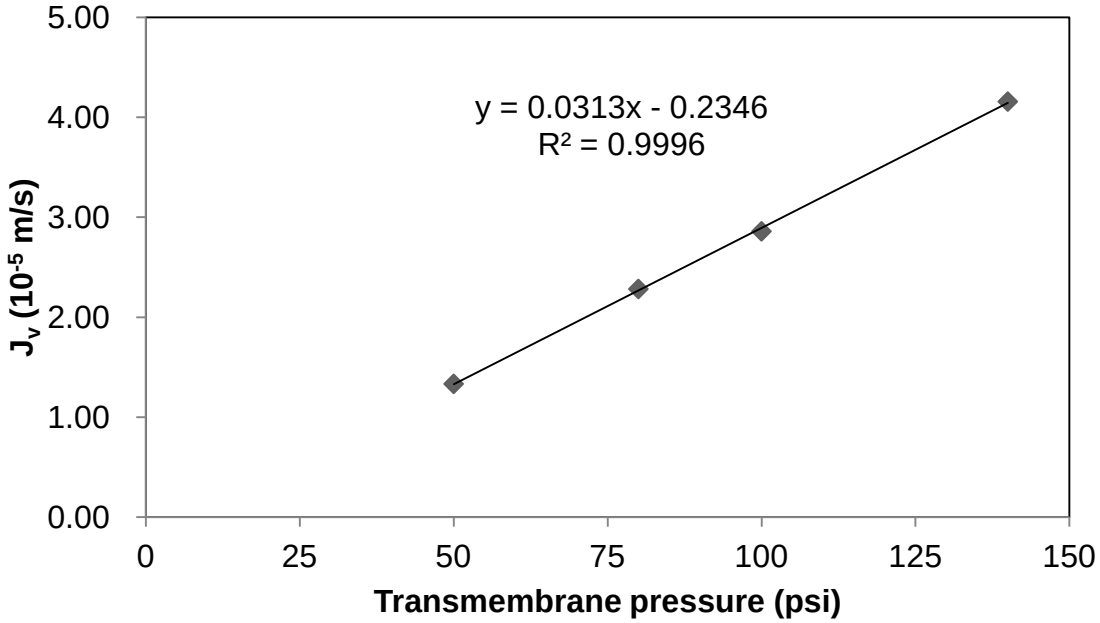

Figure 4-1-4 Solvent flux operated under various level of transmembrane pressure by NF-270 membrane at pH 3 and cross flow velocity 0.18 m/s.

The effect of transmembrane pressure on rejection is shown in Figure 4-1-5 for pH 8 and pH 3. The general trend is that rejection increases as transmembrane pressure increases, and this relationship is more obvious for acetaminophen. At pH 8, rejection of acetaminophen increases from 31% to 48% at the transmembrane pressure of 50 psi and 140 psi, respectively. Rejection of caffeine increases from 65% to 75% at the transmembrane pressure of 50 psi and 140 psi, respectively. Rejection of carbamazepine increases from 75% to 81% at the transmembrane pressure of 50 psi and 140 psi, respectively. Rejection of octylphenol increases from 58% to 67% at the transmembrane pressure of 50 psi and 140 psi, respectively. The trend of rejection at pH 3 is almost the same as that at pH 8, except for diclofenac.

For most solutes, the rejection increase because of an increase in transmembrane pressure is due to the increase of solvent flux, and slight increase of solute flux. Because the size of the solvent, water, is the smallest among all the other molecules in the solution, increasing pressure will increase the permeation of water more significantly than for other solutes, thus increasing rejection. Therefore, for smaller solutes, such as acetaminophen, increases in transmembrane pressure will increase rejection more significantly. For a solute that is hard to permeate, such as diclofenac, an increase in rejection is not obvious or do not exist.

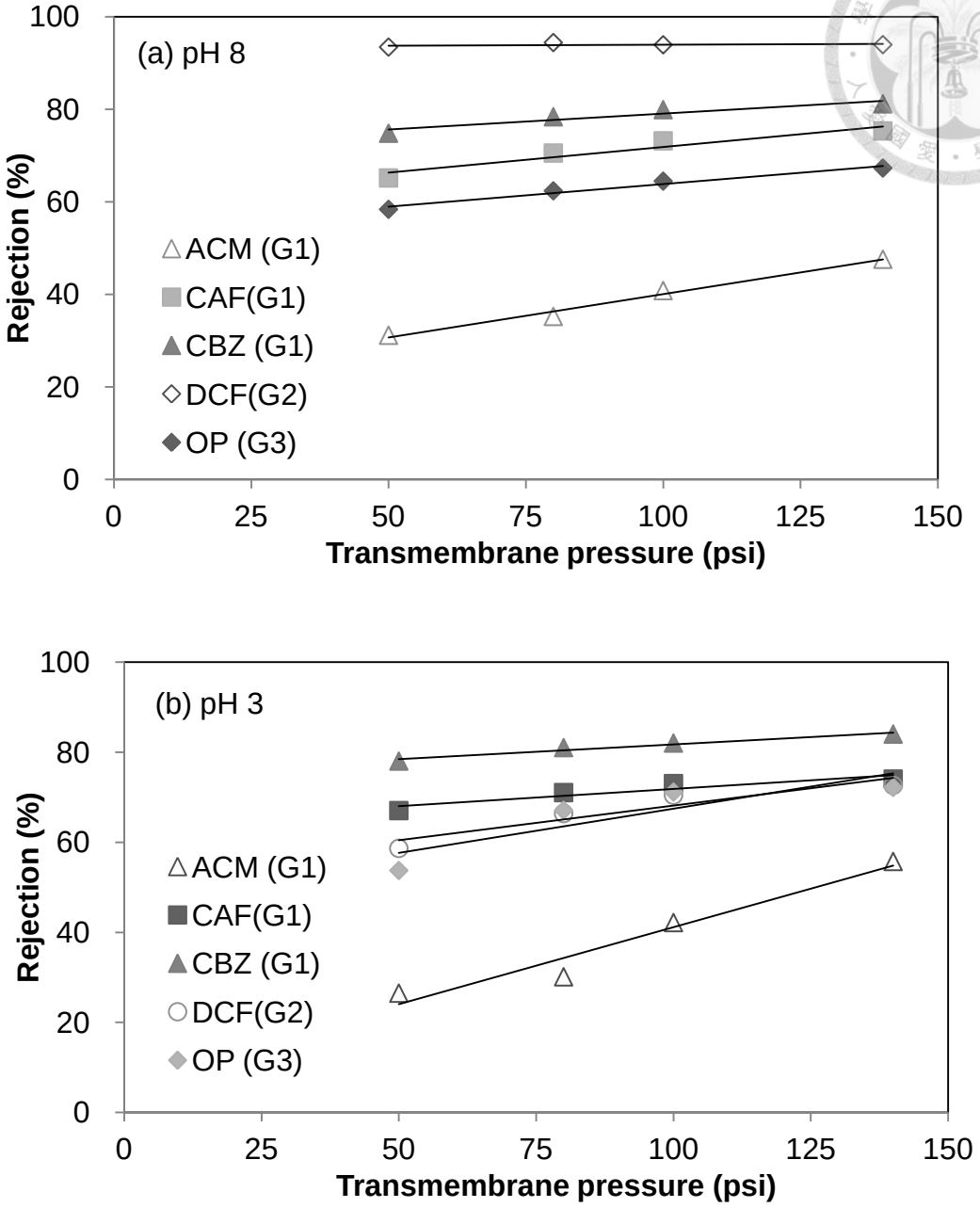

Figure 4-1-5 Rejections of mixed solutes (2 mg/L acetaminophen, caffeine, octylphenol, carbamazepine, diclofenac) by NF-270 membrane operated under various level of transmembrane pressures at pH 8 (a) and 3 (b) and cross flow velocity=0.18m/s

4-1-3 Effect of cross flow velocity on rejection

The effect of cross flow velocity on rejection is shown in Figure 4-1-6 at pH 8. The general trend is that rejection slightly increased as cross flow velocity increased from 0.09 m/s to 0.18 m/s, but rejection did not vary as cross flow velocity increased from 0.18 m/s to 0.27 m/s. For most solutes, this trend is likely caused by the effect of concentration polarization. When cross flow velocity decreases, concentration polarization will be more severe, which means that higher concentration of solutes will be on the membrane surface, thus causing the permeate concentration to increase and rejection to decrease. When cross flow velocity increases to a threshold, the concentration polarization effect will be minimized, so the difference between rejections at cross flow velocity 0.18 m/s and 0.27 m/s are not significant.

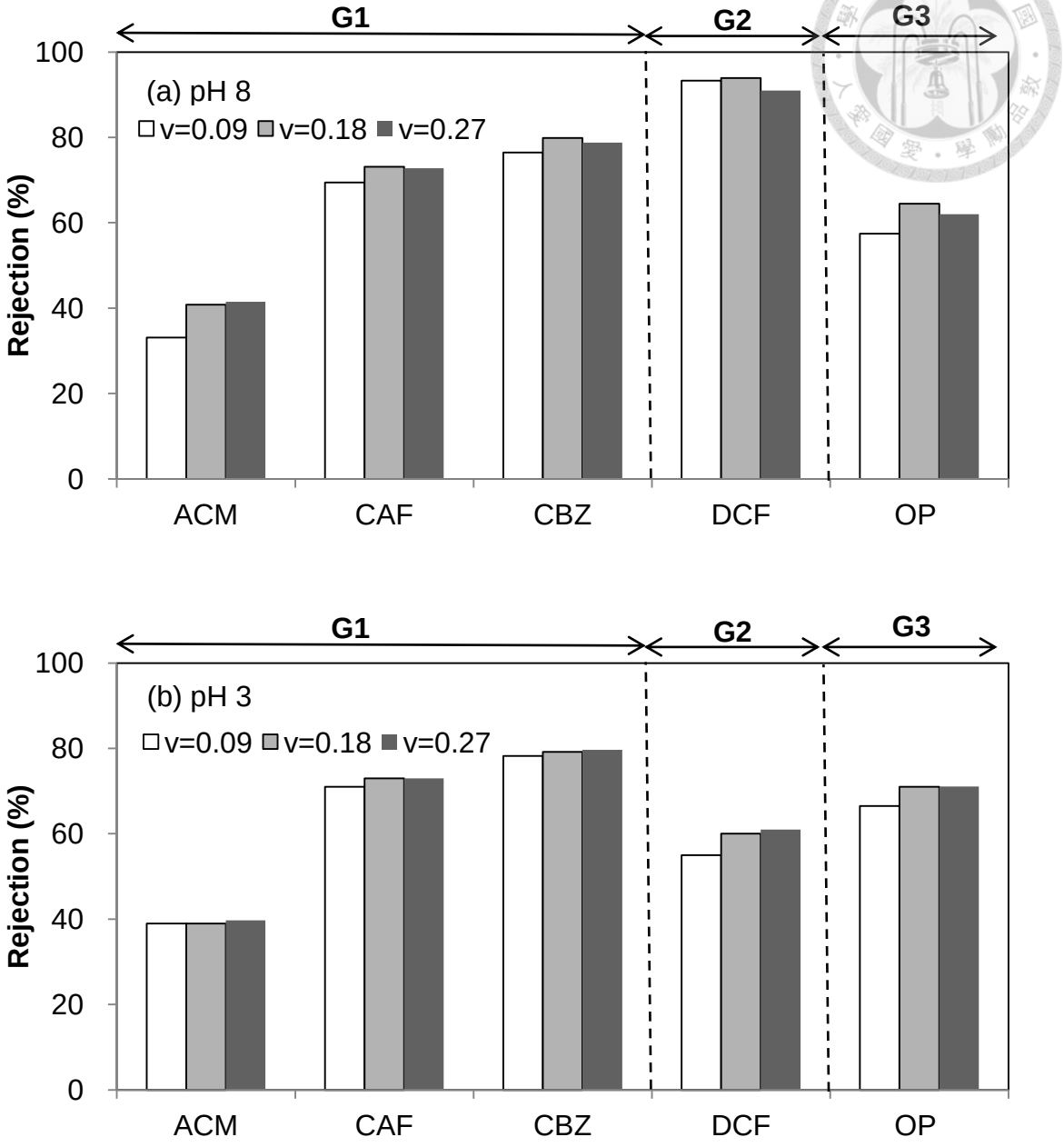

Figure 4-1-6 Rejections of mixed solutes by NF-270 membrane operated under various level of cross flow velocities, transmembrane pressure 100 psi, and at pH 8 (a) and pH 3 (b), respectively.

4-2 Differentiation of three rejection mechanisms: size exclusion, electrostatic repulsion and adsorption

4-2-1 Overall trends of rejection of target compounds

Figure 4-2-1 shows the rejection of target compounds (acetaminophen, caffeine, octylphenol, carbamazepine, sulfamethoxazole, trimethoprim, diclofenac, bisphenol A) by NF270 membrane at transmembrane pressure 100 psi, pH 8, cross flow velocity 0.27 m/s. Rejection at pH 8 for group 1 compounds are low to medium high, for group 2 compounds are high, and for group 3 compounds are low. The rejection is mainly attributed to size exclusion, but other mechanisms, such as electrostatic repulsion and adsorption still have an effect on rejection.

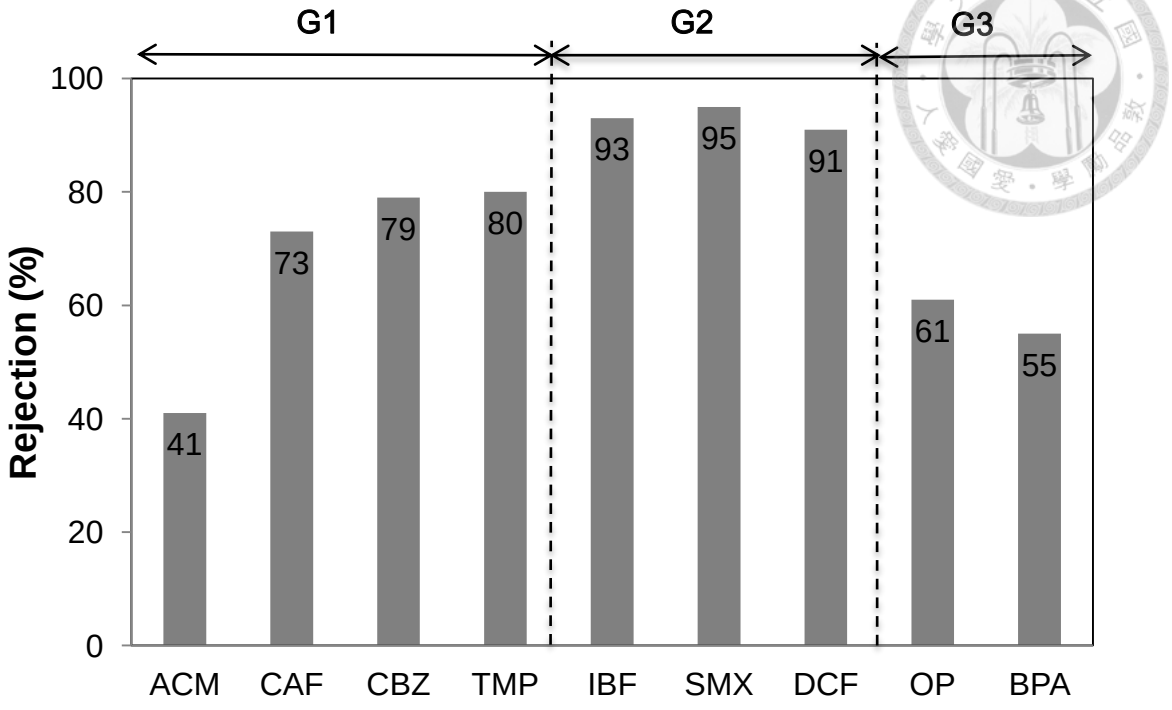

Figure 4-2-1 Rejections of target compounds by NF-270 membrane at pH 8, transmembrane pressure of 100 psi, and cross flow velocity of 0.27m/s.

4-2-2 Electrostatic repulsion

4-2-2-1 Effects of solute charges and solution's pH on rejection

Electrostatic repulsion is caused by the repulsion between a negatively charged membrane and negatively charged solutes. Therefore, electrostatic repulsion will occur for a solute that has negative charge. In other word, when the pKa of solute is smaller than the pH of solution, the solute will has negative charge and has electrostatic repulsion.

Figure 4-2-2 shows the rejections of acetaminophen, caffeine, carbamazepine, trimethoprim, ibuprofen, diclofenac, sulfamazaxole, octylphenol, and bisphenol A at pH 3 and 8. Solutes of group 1 and group 3, like acetaminophen, caffeine, carbamazepine, octylphenol and bisphenol A have similar rejection at pH 3 and 8, except for trimethoprim. On the other hand, solutes of group 2 have higher rejection at pH 8 than at pH 3, a result that can be explained by electrostatic repulsion. Because solutes of group 2, like ibuprofen, diclofenac, and sulfamazaxole, have negative charge at pH 8, and NF membrane also has negative charge, two negative charges together will cause repulsion, and result in higher rejection of group 2 solutes. However, when solution is at pH 3, the group 2 solutes are neutral (pKa = 4.4, 4.08, 5.6), so rejection is lower. Trimethoprim has positive charge at pH 3 and the surface of the NF270 membrane is likely to have some positive charge at pH 3, which is lower than pH 3.5 (isoelectric

point of NF270). Thus, there will be electrostatic repulsion, so rejection of trimethoprim is higher at pH 3 than at pH 8.

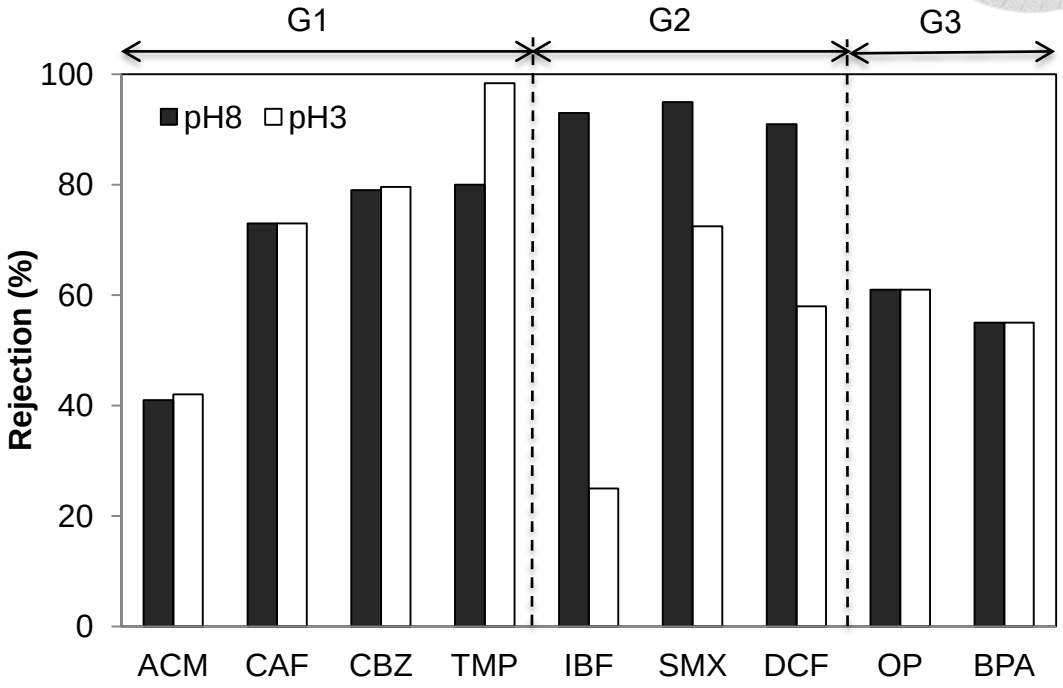

Figure 4-2-2 Rejections of mixed solutes by NF-270 membrane at transmembrane pressure of 100 psi, cross flow velocity of 0.27 m/s, and pH 3 and 8, respectively.
ACM: acetaminophen, CAF: caffeine, CBZ: carbamazepine, TMP: trimethoprim;
IBF: ibuprofen, SMX: sulfamethoxazole, DCF: diclofenac;
OP: octylphenol, BPA: bisphenol A.

4-2-2-2 Contribution of electrostatic repulsion on rejection

The extent of electrostatic repulsion can be calculated by the rejection at pH 8 minus the rejection at pH 3, and the result is shown in Figure 4-2-3. Solutes of G2 have large electrostatic repulsion effect. The contribution of electrostatic repulsion on rejection for ibuprofen, sulfamethoxazole and diclofenac are 68%, 23%, and 33%, respectively. On the other hand, solutes of G1 and G3 have nearly zero electrostatic repulsion, except for trimethoprim. Trimethoprim have electrostatic repulsion at pH 3, because it is positively charged at pH 3.

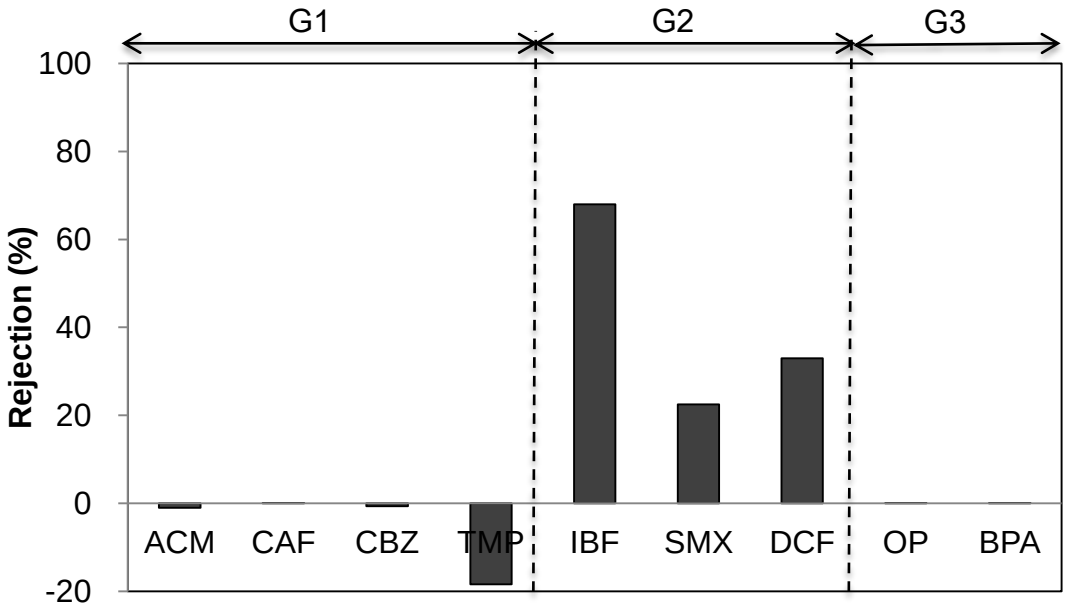

Figure 4-2-3 Contribution of electrostatic repulsion on rejection by NF270 membrane at transmembrane pressure 100 psi and cross flow velocity 0.27 m/s.

4-2-3 Adsorption

4-2-3-1 Effect of adsorption on rejection

Adsorption of solutes on NF membrane is likely due to hydrophobic interactions. Because NF membrane is more hydrophobic compared to water, hydrophobic solutes will be more likely to adsorb on NF membrane. Hydrophobicities of NF membrane can be known from the contact angle. Hydrophobicities of solutes can be known from the log K_{ow} of solute. When solute has larger log K_{ow}, it is more likely to be adsorbed on NF membrane. When solute has charge, it will become hydrophilic, making it unlikely to be adsorbed on NF membrane.

The rejections of acetaminophen, caffeine, octylphenol, carbamazepine, diclofenac at different sampling times (initial and equilibrium) at pH 3 and 8 are shown in Figure 4-2-4. Octylphenol had higher initial rejection than at final one at both pH 8 and pH 3, due to adsorption of octylphenol on the membrane surface. When adsorption capacity was exhausted, the rejection of octylphenol was decreased. Octylphenol has the highest logKow (5.28), is the most hydrophobic compound, and was strongly adsorbed on to the membrane surface. Diclofenac also had higher initial rejection at pH 3 (65%), but the rejection decreased with time and reached a final rejection (58%). Because diclofenac also has high logKow (4.51), it can adsorb on the membrane.

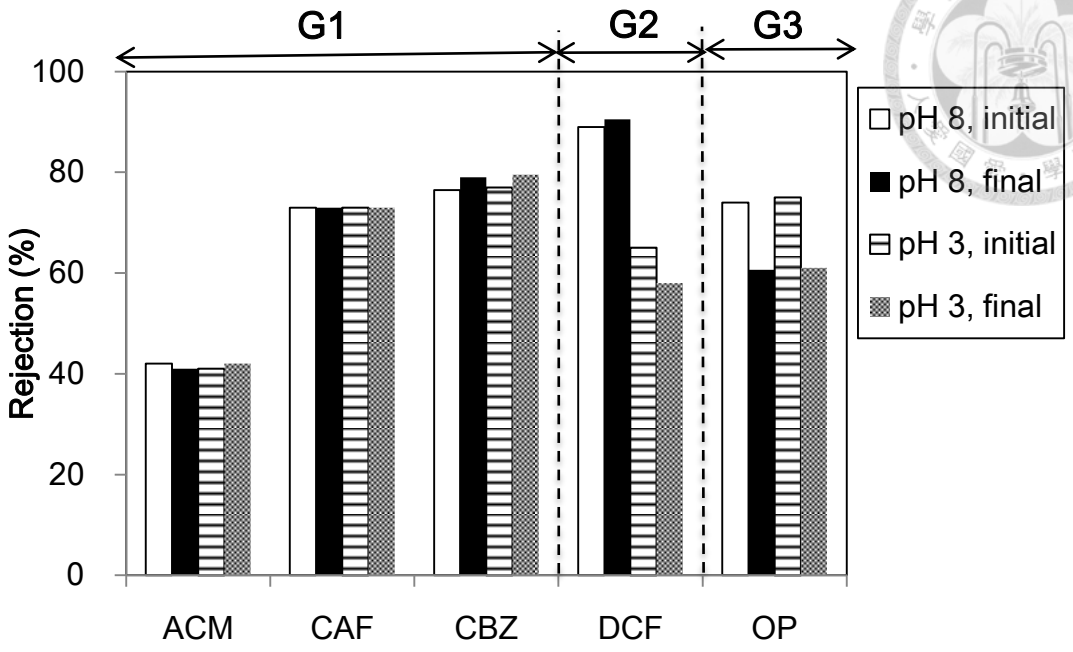

Figure 4-2-4 Rejections of mixed solutes (2 mg/L caffeine, octylphenol, carbamazepine, diclofenac) by NF-270 membrane at initial (0.5 h) and final (24 h) at pH 8 and pH 3 at transmembrane pressure 100 psi.

The change of feed concentration versus time is shown in Figure 4-2-5. The figure shows that feed concentration of caffeine and carbamazepine does not vary much with time, but octylphenol (at pH 8 and 3) and diclofenac (at pH 3) decrease remarkably. Feed concentration decreases of octylphenol and diclofenac are due to adsorption on the NF membrane, this result agrees with the above comments.

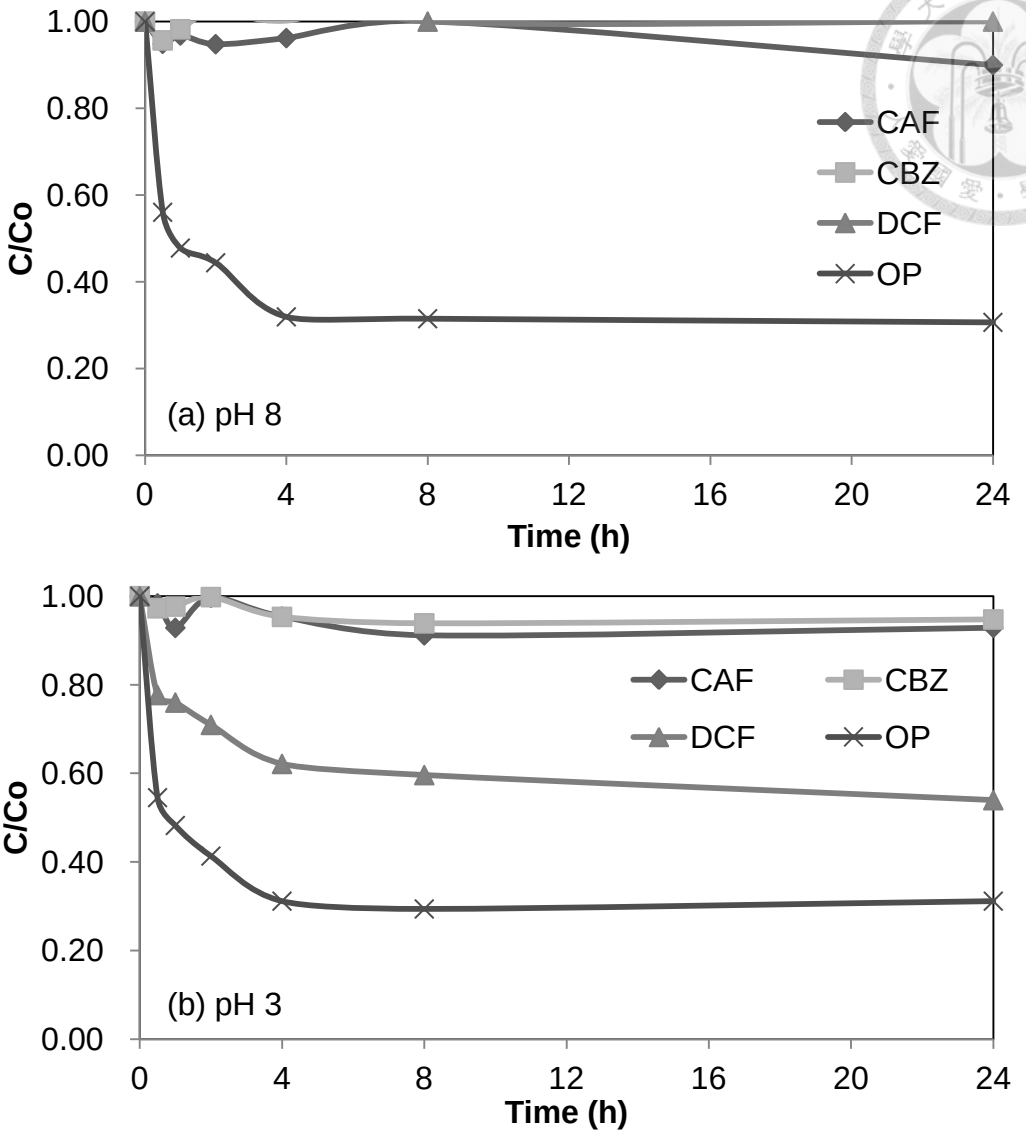

Figure 4-2-5 Residual concentration ratio of mixed solutes (2 mg/L caffeine, octylphenol, carbamazepine, diclofenac) by NF-270 membrane at transmembrane pressure of 100 psi, cross flow velocity of 0.27 m/s, and at pH 8 (a) and pH 3 (b), respectively.

4-2-3-2 Adsorption experiment to validate adsorption effect

To check the adsorption effect, adsorption experiments was conducted by using Jar test equipment. A blank sample was used to verify concentration decreases not caused by other factors. The adsorption results for selected compounds are shown in Figure 4-2-6.

The result of the blank experiment indicates that the decrease in concentration is not caused by other factors. In adsorption experiments with NF membrane, concentrations of carbamazepine and caffeine are relatively stable, showing that they have little to no adsorption effect. However, octylphenol and diclofenac show obvious concentration decreases, which is caused by adsorption. For diclofenac, concentration decrease and adsorption only occur at pH 3, showing that diclofenac is only adsorbed at pH 3 and not at pH 8. This is because diclofenac is negatively charged at pH 8, causing electrostatic repulsion. On the other hand, at pH 3, diclofenac is neutral and can be adsorbed on the membrane.

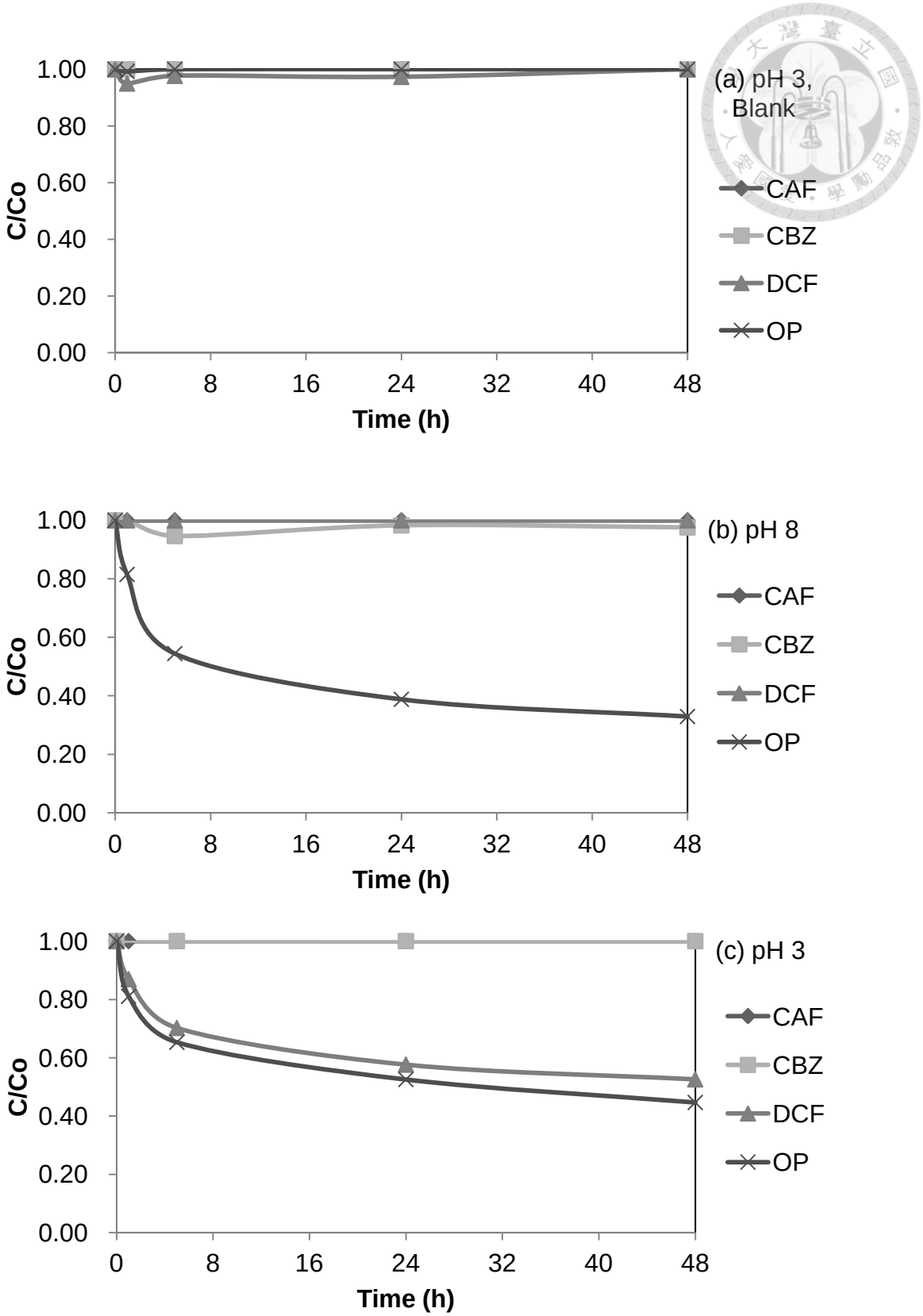

Figure 4-2-6 Residual concentration ratio on adsorption experiments of mixed compound (caffeine, carbamazepine, diclofenac, octylphenol) without NF membrane at pH 3 (a) and with NF270 membrane at pH 8 (b) and pH 3 (c).

4-2-3-3 Contribution of adsorption on rejection

The extent of adsorption can be calculated by subtracting the initial rejection and final rejection, and the result is shown in Figure 4-2-7. G3 Solutes have adsorption effect. The contribution of adsorption on rejection for octylphenol and bisphenol A are 15% and 10%, respectively. On the other hand, G1 solutes have nearly zero adsorption. For G2 solutes, ibuprofen and diclofenac have adsorption effect only at pH 3, because they are more hydrophobic at pH 3.

The contribution of adsorption on rejection versus log K_{ow} is shown in Figure 4-2-8. When log K_{ow} of solute is below 3, the effect of adsorption was not obvious or did not exist. For these hydrophilic solutes, they are more likely to stay in water environment, so they are unlikely adsorbed on membrane or the amount of adsorption are so small that can not be detected. When adsorption occurred, the extent of the contribution of adsorption on rejection increased as log K_{ow} increased, except for bisphenol A.

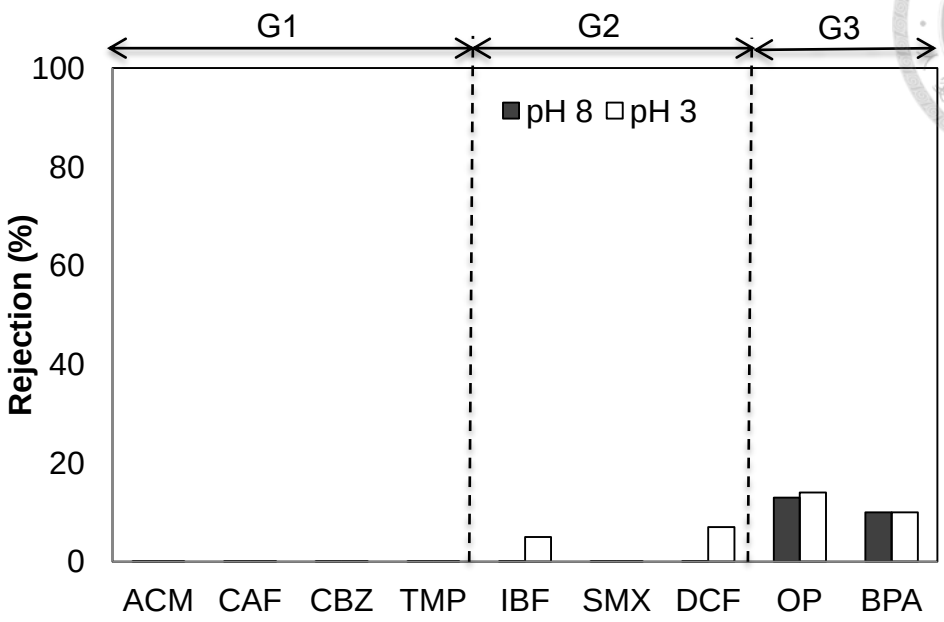

Figure 4-2-7 Contribution of adsorption on rejection by NF270 membrane at transmembrane pressure 100 psi and cross flow velocity 0.27 m/s.

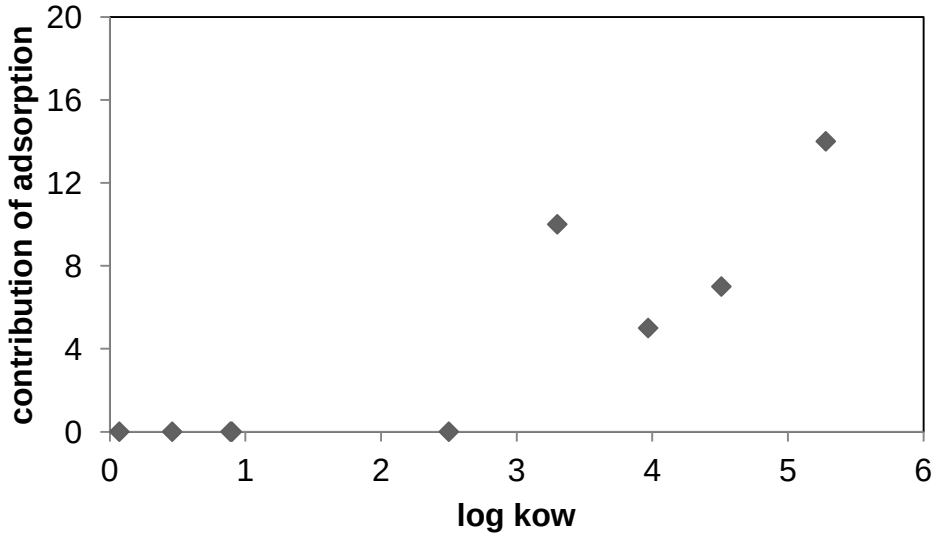

Figure 4-2-8 Contribution of adsorption on rejection versus log octanol-water partition coefficient.

4-2-4 Contribution of size exclusion on rejection

Size exclusion is the main rejection mechanism of the NF membrane. The main affecting factor is solute size. When the solute size is larger, rejection is larger.

The extent of size exclusion can be calculated from the final rejection at pH 3 or by subtracting electrostatic repulsion and adsorption effect from rejection at pH 8, and the result is shown in Figure 4-2-9. All solutes have size exclusion effect on rejection.

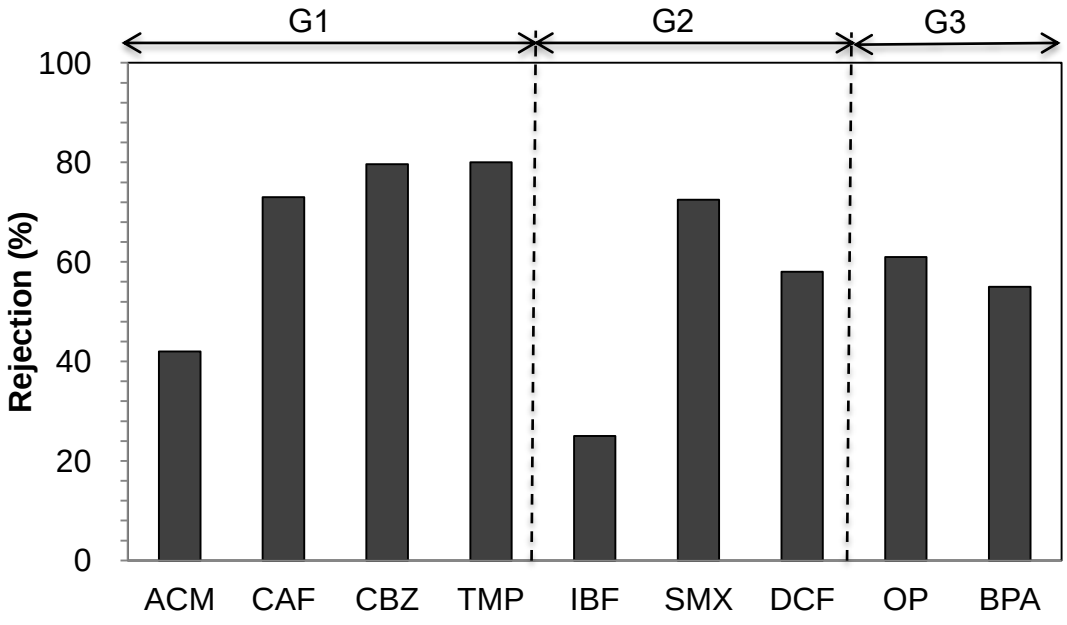

Figure 4-2-9 Contribution of size exclusion on rejection by NF270 membrane at transmembrane pressure 100 psi and cross flow velocity 0.27 m/s.

Rejection of G1 solutes by the NF270 membrane according to molecular weight or molecular volume at pH 8 is shown in Figure 4-2-10. Molecular volume is molecular weight divided by the density of the compound. The rejection of G1 solutes increased as molecular weight or molecular volume increased. The rejection of acetaminophen was the lowest (41%), followed by caffeine (75%), carbamazepine (79%), and trimethoprim (80%). Acetaminophen has the smallest molecular size (MW=151), causing rejection to be the lowest.

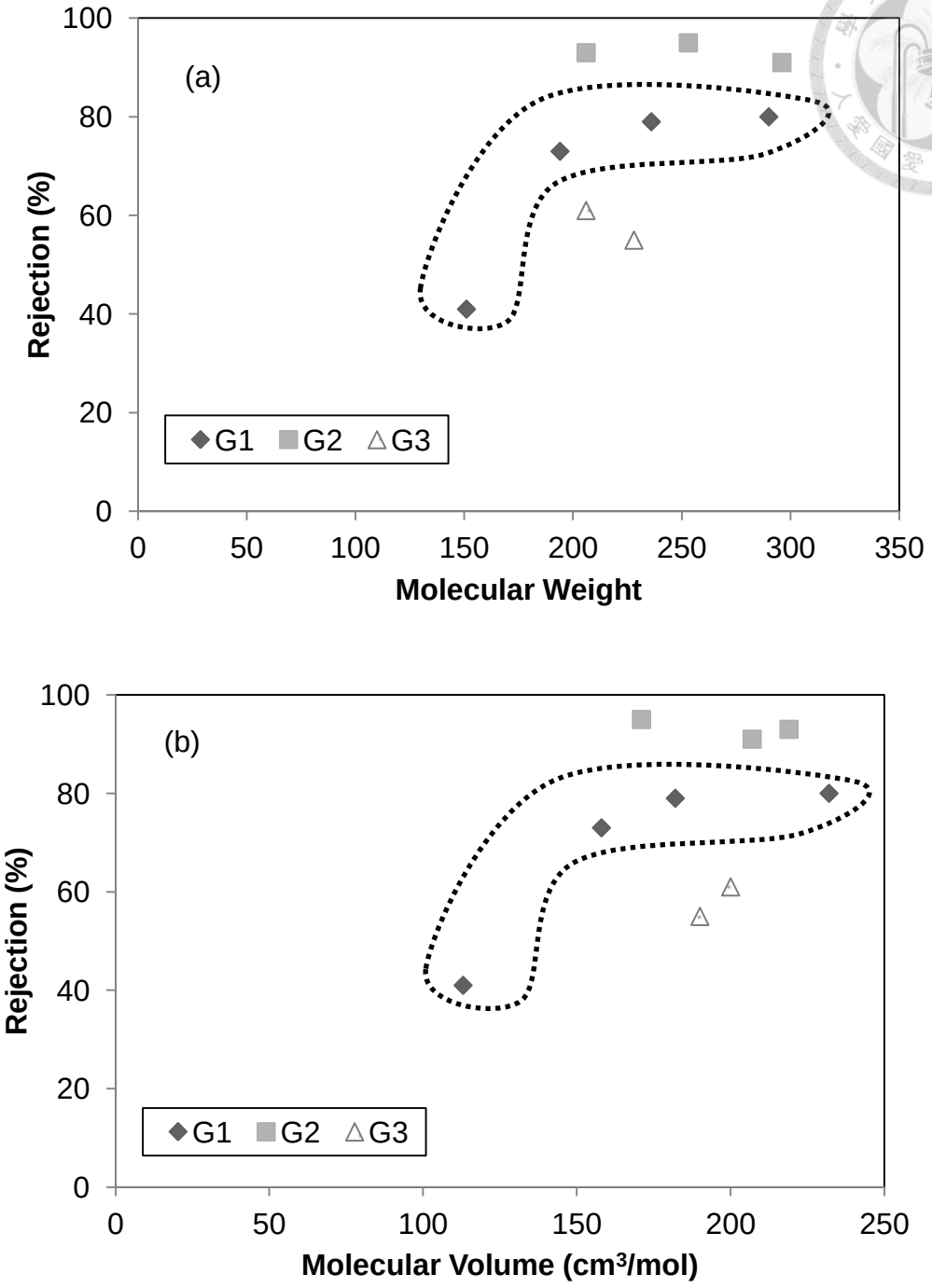

Figure 4-2-10 Rejections of G1 solutes by NF-270 membrane according to molecular weight (a) or molecular volume (b) at pH 8, transmembrane pressure 100 psi, cross flow velocity 0.27m/s

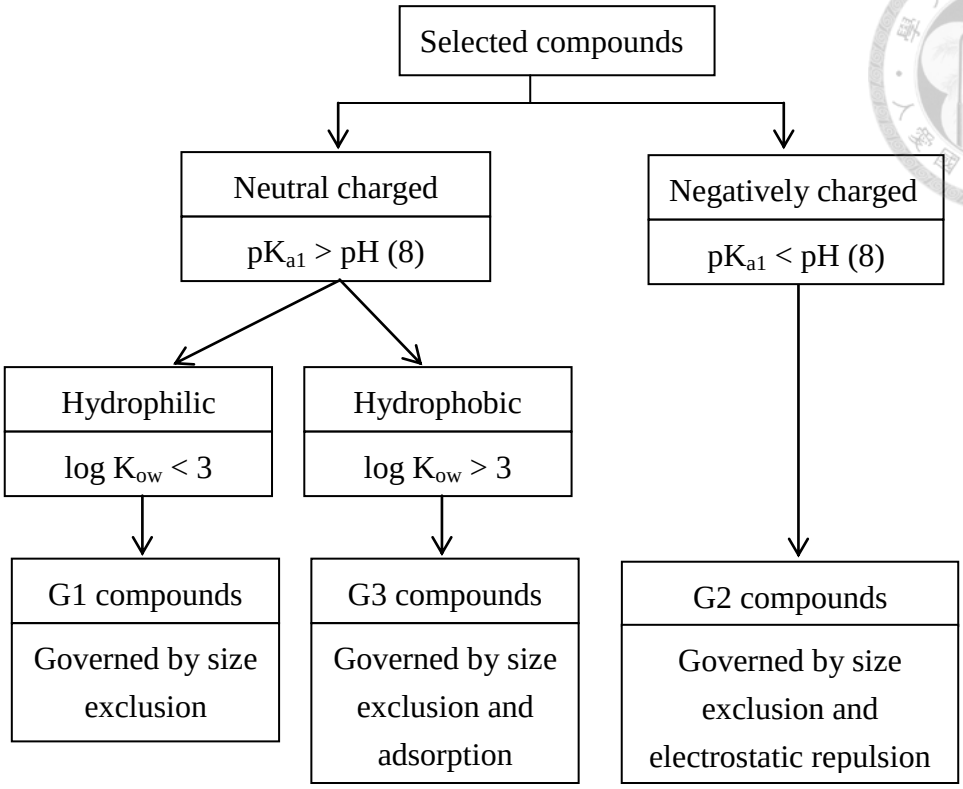

Figure 4-2-11 Flowchart of target compounds classification and governing rejection mechanisms

4-2-5 Summary of solutes rejection mechanisms

Figure 4-2-11 represents the flowchart of target compounds classification and governing rejection mechanisms.

Table 4-2-1 summarizes the extent of the three rejection mechanisms for nine solutes by the NF270 membrane. The contribution of electrostatic repulsion on rejection is calculated by the rejection at pH 3 minus the rejection at pH 8. The contribution of adsorption on rejection is calculated by the initial rejection at pH 3 minus the final rejection at pH 3. The contribution of size exclusion is calculated by subtracting electrostatic repulsion and adsorption effect from rejection at pH 8.

These results agree with the previous hypothesis on classifying target compounds into three groups. Rejection is mainly caused by size exclusion. Rejections of group 1 solutes are all governed by size exclusion. Rejections of group 2 solutes are high, and are governed by size exclusion and electrostatic repulsion. Trimethoprim is positively charged at pH 3, so it has electrostatic repulsion. Ibuprofen and diclofenac only have adsorption effect at pH 3 because they are more hydrophobic. It can be concluded that electrostatic repulsion and adsorption effect can not coexist simultaneously. Rejections of solutes of group 3 are governed by size exclusion and adsorption. Although they have higher rejection initially, they have lower rejection at equilibrium compared with similar sized solutes.

Table 4-2-1 Summary of contribution of three rejection mechanisms

Compound	Group	MW	pKa	log Kow	SE	ER	AD	Total
Acetaminophen	G1	151	14	0.07	40	0	0	40
Caffeine	G1	194	9.5	0.46	75	0	0	75
Carbamazepine	G1	236	13.9	2.5	80	0	0	80
Trimethoprim	G1	290	17.3, 7.1	0.9	78	0**	0	78
Ibuprofen	G2	206	4.4	3.97	25	68	0*	93
Sulfamethoxazol	G2	253	5.6	0.89	72	23	0	95
Diclofenac	G2	296	4.08	4.51	58	33	0*	91
Octylphenol	G3	206	10.3	5.28	61	0	14	76
Bisphenol A	G3	228	10.3	3.3	55	0	10	65

*At pH 3, ibuprofen has adsorption effect of 5%, and diclofenac has 7%.

**At pH 3, trimethoprim has 20% of electrostatic repulsion effect.

Figure 4-2-12 is another way to represent the extent of the three rejection mechanisms for nine solutes by the NF270 membrane.

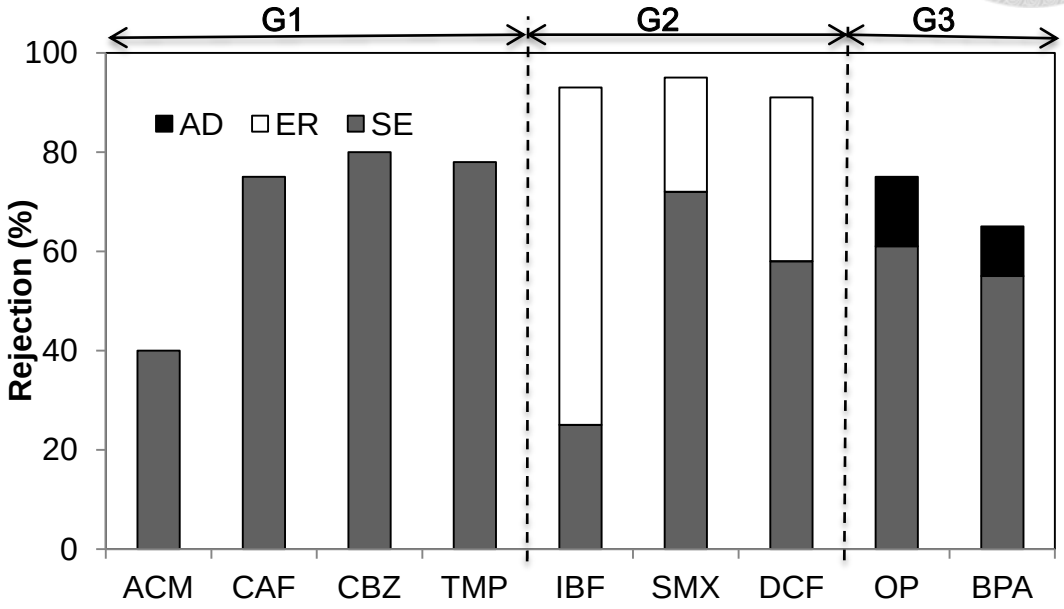

Figure 4-2-12 Summary of contribution of three rejection mechanisms at transmembrane pressure of 100 psi, cross flow velocity of 0.27m/s and at (a) pH 3 and (b) pH 8, respectively.

4-3 Elucidation of the NF membrane rejection model

4-3-1 Determination of common model parameters

The value of equipment parameters are listed in table 4-3-1.

Table 4-3-1 Equipment parameter's value

Symbol	Name	Value	Unit	Value obtained
l	channel length	0.146	m	provided by manufacturer
h	channel height	0.002	m	provided by manufacturer
w	channel width	0.095	m	provided by manufacturer
dh	hydraulic diameter	0.0040	m	$2\times wh/(w+h)$
As	surface area	0.01387	m^2	$l\times w$
Ac	cross-sectional area	0.00019	m^2	$w\times h$
T	water temperature	295	K	measured
ρ	water density	999.9	kg/m^3	known
μ	water viscosity	9.58×10^{-4}	kg/ms	known
Q_f	feed flow rate	2100	mL/min	measured
Q_p	permeate flow rate	18	mL/min	measured
ΔP	transmembrane pressure	6.90×10^5	N/m^2	measured
v	cross flow velocity	0.1842	m/s	Q_f/A_c
J_v	solvent flux	2.16×10^{-5}	m/s	Q_p/A_s
$\Delta x/\varepsilon$	ratio of membrane thickness to porosity	7.69×10^{-7}	m	eq. 3-16
r_p	membrane pore radius	4.30×10^{-10}	m	provided by manufacturer

Common parameters of solutes are shown in table 4-3-2.

Table 4-3-2 Common parameters of solutes

Name	Acetaminophen	Caffeine	Sulfamethoxazol	Carbamazepine	Bisphenol A	Ibuprofen	Diclofenac	Octylphenol	Trimethoprim
MW	151	194	253	236	228.3	206	296	206	290
$\rho(g/cm^3)$	1.34	1.23	1.478	1.296	1.2	1.03	1.432	0.94	1.252
$Va(cm^3/mol)$	112.7	157.7	171.2	182.1	190.3	200.0	206.7	219.1	231.6
Ds(m/s)	8.6E-10	7.1E-10	6.73E-10	6.49E-10	6.3E-10	6.1E-10	6.0E-10	5.8E-10	5.6E-10
Re	1135	1135	1135	1135	1135	1135	1135	1135	1135
Sc	1113	1356	1423	1476	1515	1560	1591	1646	1701
Sh	177	186	188	190	191	192	193	195	197
Kf	$3.8\ 10^{-5}$	3.3×10^{-5}	3.2×10^{-5}	3.1×10^{-5}	3.0×10^{-5}	3.0×10^{-5}	2.9E-05	2.8E-05	2.8E-05
β	1.765	1.933	1.980	2.018	2.046	2.079	2.101	2.142	2.183

The important parameters for determining rejection are solute sizes and diffusion coefficients. Solute size is represented by molar volume (V_a) or solute radius, and it is dependent on molecular weight and the solute's density. Solutes with lower molecular weight typically have smaller size. Octylphenol has a larger molecule size because it has a lower density. Sulfamethoxazol and diclofenac have a higher density, resulting in a smaller size. Diffusion coefficient is dependent on molar volume and solvent viscosity. When molar volume is larger, diffusion coefficient is smaller.

The Reynolds number (Re) is a dimensionless number that gives a measure of the ratio of inertial forces to viscous forces. The Schmidt number is a dimensionless number defined as the ratio of momentum diffusivity (viscosity) and mass diffusivity. The Sherwood number (Sh) represents the ratio of convective to diffusive mass transport. The Re of all solutes are the same because it represents the flow condition. However, Sc and Sh are not the same for all solutes because they are affected by the diffusion coefficient (D_s). When Ds is small, Sc and Sh are large, which means that solute diffusive mass transport is small compared to viscosity and convective mass transport. The mass transfer coefficient is dependent on Sherwood number and diffusion coefficient. When solute is small, mass transfer coefficient will be small. The larger solute will have larger mass transfer coefficient, hence hydrodynamic concentration polarization is more dominant.

4-3-2 Irreversible thermodynamics model for uncharged solutes

Predicted rejection by an irreversible thermodynamics model can be calculated by:

$$R_r = \frac{\sigma[(1 - \exp(pe)]}{1 - \sigma \exp(pe)} \qquad (3-4)$$

β is the hydrodynamic concentration polarization factor, R is the observed rejection.

Table 4-3-3 shows the result of the rejection predicted by the irreversible thermodynamics model. This predicted rejection by the irreversible thermodynamics model only considers the effect of size exclusion. Size exclusion is considered the main retention mechanism because it accounts for a large proportion of rejection.

The ratio of solute to pore radius λ_1 for all solutes are larger than 0.8. For smaller solutes with smaller λ_1, they have lower reflection coefficient σ and lower solute permeability P. Some solutes have λ_1 that are larger than 1. Application of SHP model to such large molecules are not appropriate because its calculation is mainly based on $(1-\lambda)^2$.

The comparison between the experimental rejection and predicted rejections is shown is Figure 4-3-1. The predicted rejections of small solutes are underestimated. For example, the rejections of acetaminophen and caffeine are lower than those of the experimental results. On the other hand, the predicted rejection of bigger solutes is overestimated. For example, the predicted rejections of carbamazepine and trimethoprim are higher than those of the experimental results.

Table 4-3-3 Comparison of predicted rejection (R_{pr}) and experiment rejection (R_{ex}) by the irreversible thermodynamics model

Name	Acetaminophen	Caffeine	Sulfamethoxazol	Carbamazepine	Bisphenol A	Ibuprofen	Diclofenac	Octylphenol	Trimethoprim
rs1	3.55E-10	3.97E-10	4.16E-10	4.51E-10	4.08E-10	4.30E-10	4.34E-10	4.23E-10	4.43E-10
λ1	0.825	0.923	0.968	*1.049*	0.949	0.999	*1.010*	0.983	*1.030*
σ	0.867	0.970	0.995	0.986	0.986	1.000	0.999	0.998	0.995
P	3.42E-05	5.43E-06	8.41E-07	1.78E-06	2.31E-06	5.29E-10	8.20E-08	2.47E-07	6.86E-07
Pe	8.41E-02	1.18E-01	1.37E-01	1.74E-01	1.28E-01	1.50E-01	1.55E-01	1.43E-01	1.65E-01
Rpr(IT)	23	65	92	83	81	100	99	98	93
Rex (pH 3)	42	75	80	80	72	25	58	55	61
RPI	59%	14%	14%	4%	12%	120%	52%	56%	42%

RPI= $|R_{pr}-R_{ex}| / 0.5(R_{pr}-R_{ex})$

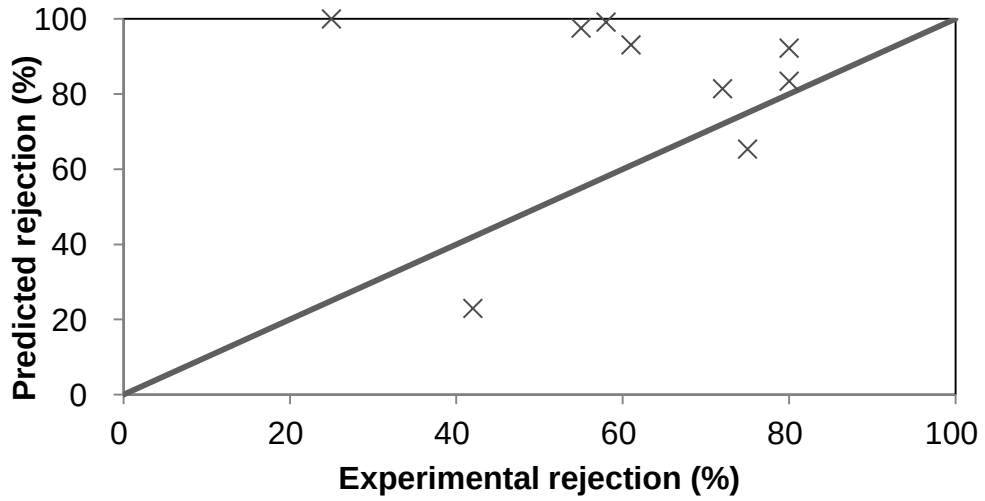

Figure 4-3-1 Comparison between experimental rejection and predicted rejection by the irreversible thermodynamics model

4-3-3 Extended Nerst-Planck model for uncharged solutes

Predicted rejection by the extended Nerst-Planck model can be calculated by:

$$R = 1 - \frac{\beta\varphi K_c}{1 - \left((1 - \varphi K_c)\exp(-Pe)\right) - \varphi K_c((1 - \beta)} \qquad (3-9)$$

Table 4-5-4 shows the predicted rejection using the extended Nerst-Planck model. Solutes are sorted according to the solute radius. The predicted rejection only considered the effect of size exclusion because size exclusion is the main mechanism contributing to rejection.

In this model, all λ_2 is smaller than 1. For smaller solutes with smaller λ_2, the solutes will have larger Kc and Kd, but smaller φ. The comparison between the experimental rejection and predicted rejections is shown is Figure 4-3-2. Results show that the predicted rejection for relatively small solutes such as acetaminophen and caffeine are similar to the experimental rejections, but for larger solutes the predicted rejection is overestimated. Similar overestimation was reported in the literature (Verliefde et al., 2009).

The lower rejections in experiments with octylphenol and bisphenol A may be due to adsorption effect. When solutes adsorbed on the membrane, they are more likely to diffuse across membrane pores, thus leading to lower rejection.

The predicted rejection by the irreversible thermodynamics model is different

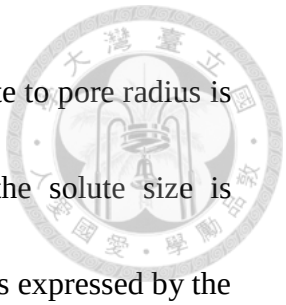

than that by the extended Nerst-Planck model. First, the ratio of solute to pore radius is expressed in two ways depending on solute radius: λ_1, where the solute size is measured by the hydrodynamic radius, and λ_2, where the solute size is expressed by the Stokes radius. All λ_2 are smaller than λ_1, because the Stokes radius is smaller than the hydrodynamic radius. This will result in predicted rejection by the irreversible thermodynamics model that is lower than that by the extended Nerst-Planck model. Second, even with the same size, the predicted rejection is lower for the irreversible thermodynamics model because the calculated steric hindrance is higher for irreversible thermodynamics model.

Table 4-3-4 Comparison of predicted rejection (R_{pr}) and experiment rejection (R_{ex}) by the extended Nerst-Planck model

Name	Acetaminophen	Caffeine	Carbamazepine	Trimethoprim	Sulfamethoxazol	Ibuprofen	Diclofenac	Bisphenol A	Octylphenol
rs2	2.62E-10	3.19E-10	3.47E-10	4.00E-10	3.35E-10	3.67E-10	3.74E-10	3.56E-10	3.87E-10
λ2	0.609	0.742	0.807	0.930	0.779	0.853	0.870	0.829	0.901
Kc	1.415	1.308	1.240	0.667	1.271	1.113	1.044	1.192	0.877
Kd	0.078	0.020	0.013	0.006	0.015	0.011	0.010	0.012	0.009
φ	0.153	0.067	0.037	0.005	0.049	0.022	0.017	0.029	0.010
Pe	0.350	1.518	2.412	3.037	2.161	2.677	2.761	2.557	2.900
Rpr(ENP)	38	81	90	99	87	95	96	93	98
Rex (pH 3)	42	75	80	80	72	25	58	55	61
RPI2	11%	8%	12%	21%	19%	117%	49%	51%	47%

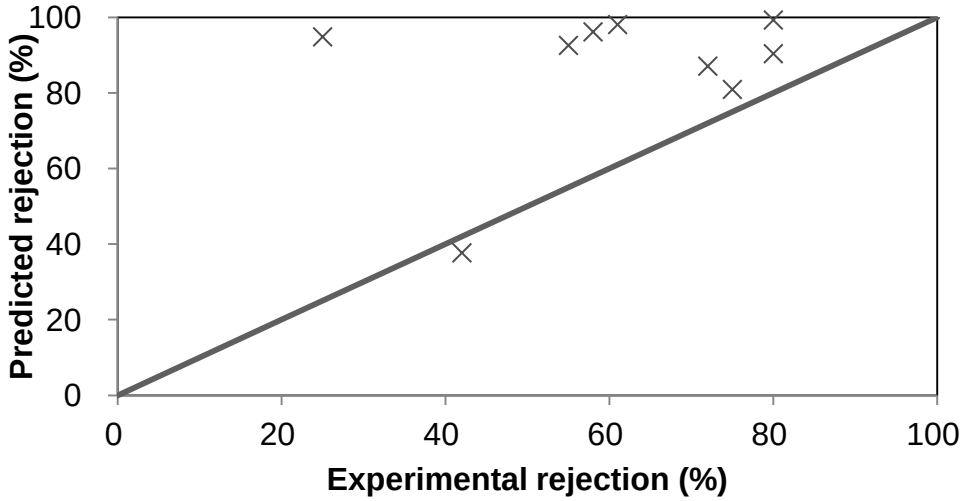

Figure 4-3-2 Comparison between experimental rejection and predicted rejection by the extended Nerst-Planck model

4-3-4 Extended Nerst-Planck model for charged solutes

The extended Nerst-Planck model for charged solutes is similar to that of charged solutes, but it adds a parameter β_{charge}. The rejection for charged solutes is:

$$R = 1 - \frac{\beta_{charge}\beta\varphi K_c}{1 - \left((1 - \varphi K_c)\exp(-Pe)\right) - \varphi K_c((1 - \beta)} \qquad (3-11)$$

$$\beta_{charge} = \exp(-Z_m \Psi F/RT) \qquad (3\text{-}12)$$

For the nanofiltration membrane NF270, at pH 8 and with 20 mM ionic strength, the zeta potential is -20 mV.

This model considers both the size exclusion and electrostatic repulsion mechanisms. Only G2 solutes, such as ibuprofen, sulfamethoxazol, and diclofenac, have negative charge at pH 8, so they have electrostatic repulsion effect.

The comparison between the experimental rejection and predicted rejections is shown is Figure 4-3-2. The predicted rejection of G2 solutes is quite fitted to experimental rejection, because the model takes both the size exclusion and electrostatic repulsion mechanisms into consideration.

Table 4-3-5 Comparison of predicted rejection (R_{pr}) and experiment rejection (R_{ex}) by charged extended Nerst-Planck model

	G1				G2			G3	
Name	Acetaminophen	Caffeine	Carbamazepine	Trimethoprim	Sulfamethoxazol	Ibuprofen	Diclofenac	Bisphenol A	Octylphenol
Zm	0	0	0	0	1	1	1	0	0
β_{charge}	1.000	1.000	1.000	1.000	0.455	0.455	0.455	1.000	1.000
R(charged)	38	81	90	99	94	98	98	93	98
Rex (pH 8)	41	75	79	80	95	93	91	55	61
RPI	8%	8%	13%	21%	1%	5%	8%	51%	47%

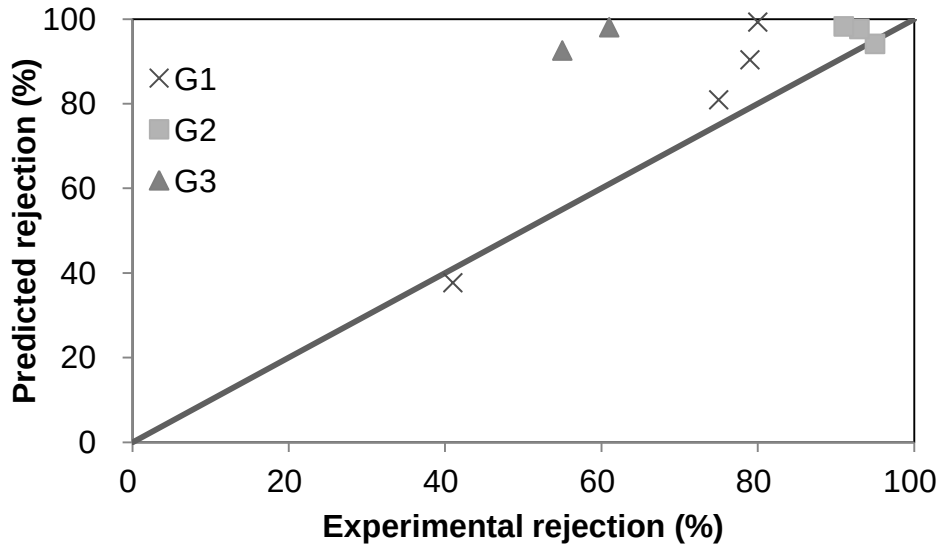

Figure 4-3-3 Comparison between experimental rejection and predicted rejection by the charged extended Nerst-Planck model

4-3-5 Model sensitivity test

4-3-5-1 Predicted effect of pore radius

The calculated rejection value is based on NF270 membrane pore radius equaling 0.43 nm. Figure 4-3-4 shows the experimental rejection and the predicted rejection with various nanofiltration membrane pore radii. It shows that the rejection increases as membrane pore radius decreases. For acetaminophen (low rejection), predicted rejection is more accurate for membrane pore radius of 0.43 nm. For caffeine, predicted rejection is more accurate for membrane pore radius of 0.45 nm. For carbamazepine, predicted rejection is more accurate for membrane pore radius of 0.45 nm. Changing the membrane pore size may fit some compounds well. However, it is not suitable for all compounds.

The model considers the membrane pore radius as uniform. The predicted rejection increases as solute size increases. When the solute has nearly the same size as the membrane pore radius, the rejection will reach nearly 100%. However, the membrane pore radius is not uniform. There can be different pore sizes along the membrane. For relatively small sized solutes, this non-uniform characteristic may not have an effect on rejection. However, for solutes that are nearly the same size as membrane pore size, the solutes will pass through the relatively bigger size of the membrane pore, causing lower rejection as the model predicted.

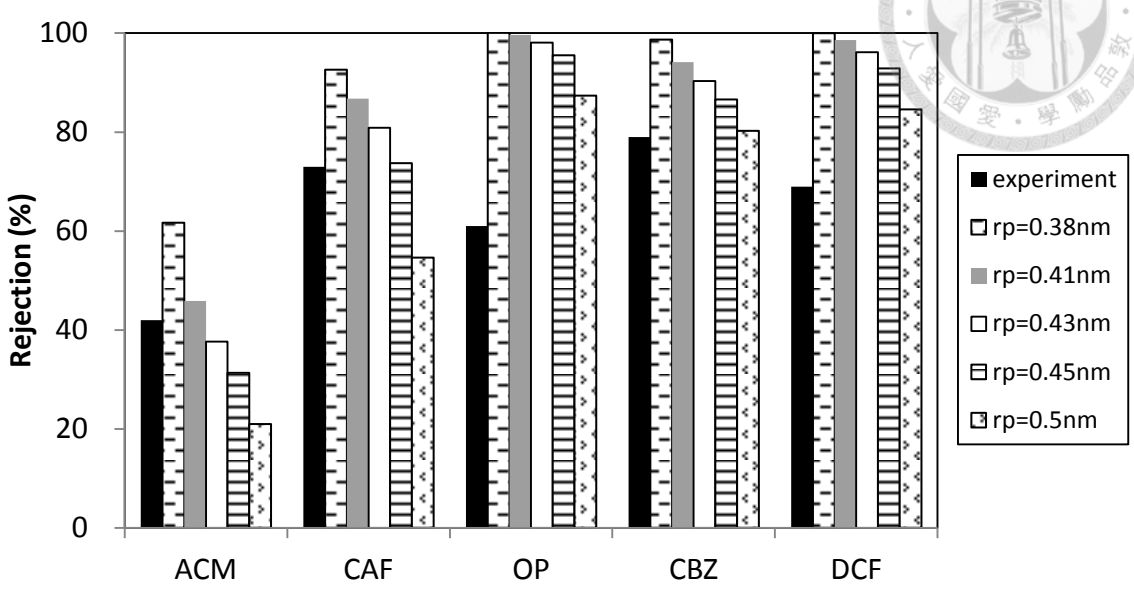

Figure 4-3-4 Compared experimental rejection and predicted rejection with various nanofiltration membrane pore radii

4-3-5-2 Effect of steric hindrance factors

There are other methods to calculate the steric hindrance factors Kc, Kd. Bungay and Brenner (1973) mentioned accurate steric hindrance factors calculation for Kc, Kd:

$$K_t = [31.4(1-\lambda)^{-2.5}][1 -1.217*(1-\lambda) +1.53*(1-\lambda)^2]$$

$$-22.51 -5.6117\lambda -0.336\lambda^2 -1.216\lambda^3 +1.647\lambda^4 \quad (4\text{-}14)$$

$$K_s = [31.4(1-\lambda)^{-2.5}][1 +0.117*(1-\lambda) -0.044*(1-\lambda)^2]$$

$$+4.018 -3.9788\lambda -1.9215\lambda^2 +4.392\lambda^3 +5.006\lambda^4 \quad (4\text{-}15)$$

$$K_{c2} = K_s / 2K_t \quad (4\text{-}16)$$

$$K_{d2} = 6л/K_t \quad (4\text{-}17)$$

Dechadilok and Deen (2006) mentioned that steric hindrance factors can be calculated as follows:

For hindrance factors for slit geometry:

$$K_{c3} = (1-3.02\lambda^2+5.776\lambda^3-12.3675\lambda^4+18.9775\lambda^5-15.2185\lambda^6+4.8525\lambda^7)/ (1-\lambda) \quad (4\text{-}18)$$

$$K_{d3} = (1+0.5625\lambda\ln\lambda-1.1936\lambda+0.4285\lambda^3-0.3192\lambda^4+0.0843\lambda^5)/(1-\lambda) \quad (4\text{-}19)$$

For hindrance factors for cylindrical geometry:

$$K_{c4} = (1+3.867\lambda-1.907\lambda^2-0.834\lambda^3)/(1+1.867\lambda-0.741\lambda^2) \quad (4\text{-}20)$$

$$K_{d4} = (1+1.125\lambda\ln\lambda-1.5603\lambda+0.52815\lambda^2+1.9152\lambda^3-2.819\lambda^4+0.2708\lambda^5+1.10115\lambda^6 -0.43593\lambda^7) / (1-\lambda)^2 \quad (4\text{-}21)$$

Different predicted rejection is shown in Figure 4-3-4. R1~R4 are rejections predicted by the extended Nerst-Planck model by different Kc, Kd for unity concentration polarization factor, calculated by eq. 4-12 and 4-13, eq. 4-16 and 4-17, eq. 4-18 and 4-19, and eq.4-20 and 4-21, respectively. The predicted rejections of R1, R2, and R4 only show slight differences. The predicted rejections for R3 are different from the others, because it is suitable for slit geometry. The rejection for small and medium sized solutes (acetaminophen and caffeine) is more suitable for cylindrical geometry. For larger solutes, the predicted rejection is overestimated.

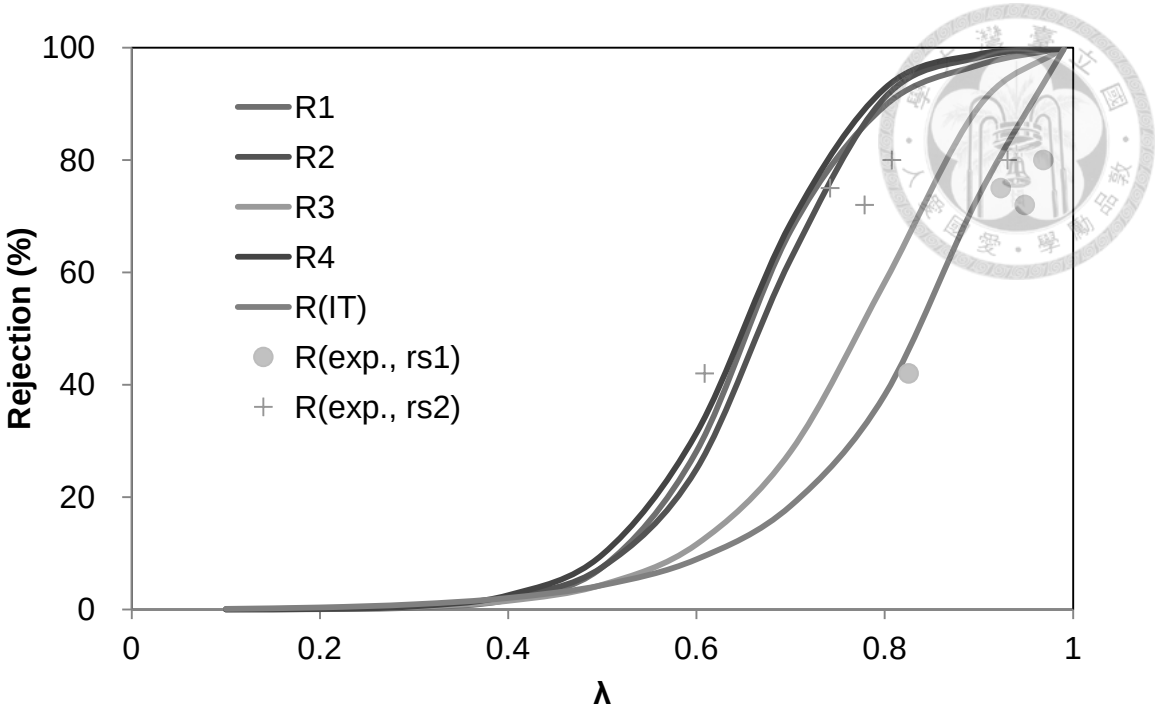

Figure 4-3-5 Comparison of predicted and experimental rejections of NF270 membrane by extended Nerst-Planck model.

R (IT): rejection predicted by irreversible thermodynamics model.

R(exp., rs1): experimental rejection, λ is calculated according to hydrodynamic radius

R(exp., rs2): experimental rejection, λ is calculated according to stokes radius

4-3-5-3 Effect of hydrodynamic concentration polarization factor

Figure 4-3-6 shows the predicted rejection at different hydrodynamic concentration polarization factors. Rejection increases as the ratio of solute to pore radius increases. An increase in hydrodynamic concentration polarization factor means that the concentration near the NF membrane is higher than in the bulk solution, so the observed rejection will be lower. The decrease in rejection has larger effect at medium ratio of solute to pore radius.

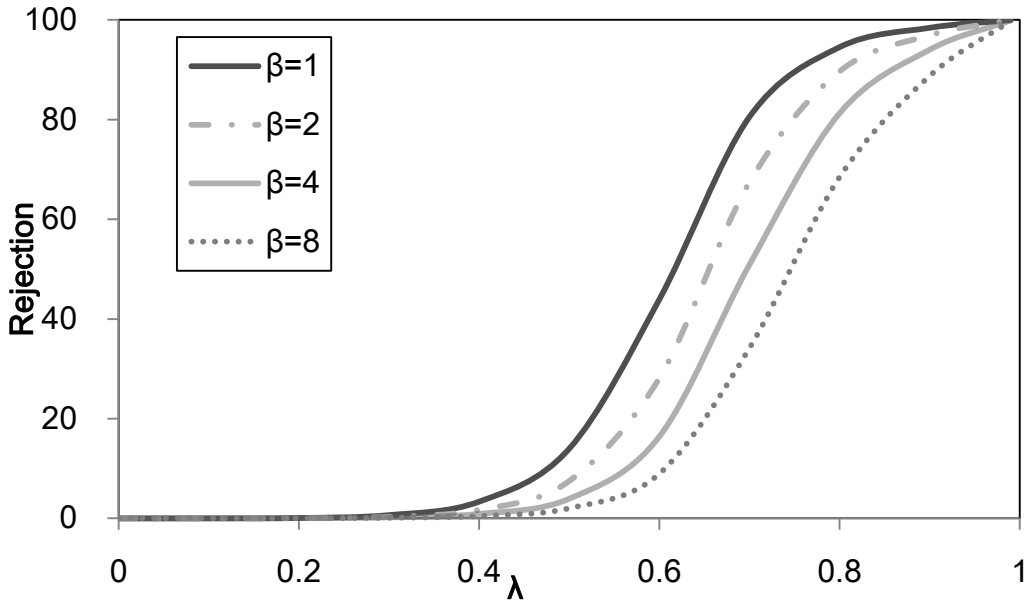

Figure 4-3-6 Predicted rejection versus ratio of solute to pore radius at different hydrodynamic concentration polarization factors

4-3-5-4 Predicted effect of cross flow velocity

Figure 4-3-7 shows the predicted rejection at different cross flow velocities. Rejection decreases significantly as cross flow velocity decreases, especially at low cross flow velocities. The decrease in rejection is likely due to the concentration polarization effect. That is, the concentration of solutes at the membrane is higher than in the bulk solution. When cross flow velocity decreases, the solute is more likely to accumulate at membrane, thus increasing the concentration polarization effect and decreasing rejection. The concentration polarization factors calculated by the model for different solutes at different cross flow velocities are shown in table 4-3-6. Results show strong concentration polarization effect at low cross flow velocities such as 0.09 m/s.

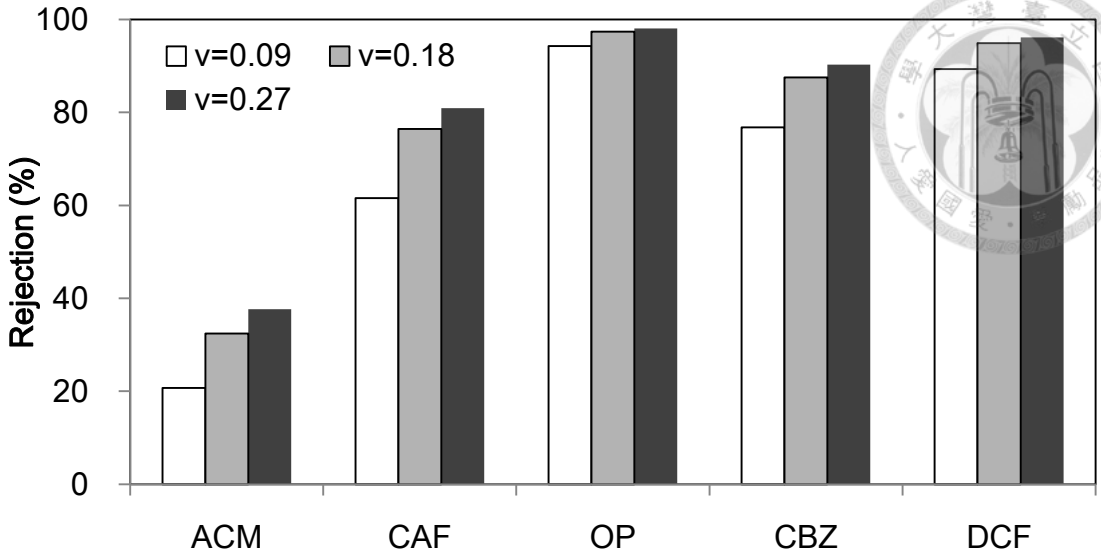

Figure 4-3-7 Predicted rejection at different cross flow velocities at transmembrane pressure 100 psi and pH 8.

Table 4-3-6 Concentration polarization factor β at different cross flow velocities

β	ACM	CAF	OP	CBZ	DCF
v=0.09	4.08	5.11	6.60	5.69	6.29
v=0.18	2.22	2.53	2.92	2.68	2.84
v=0.27	1.76	1.93	2.14	2.02	2.10

When the predicted rejection at different cross flow velocities is compared to the experimental rejection, there is a strong inconsistency. Figure 4-3-8 shows the predicted rejection versus the experimental rejection at different cross flow velocities. Even though the predicted rejection of some solutes fit the experimental rejection quite well, such as acetaminophen, the predicted rejection deviates from the experimental rejection at low cross flow velocity. Rejection does not vary significantly at different cross flow velocities, so the concentration polarization factor may not play a significant role in rejection, although cross flow velocity does affect rejection slightly.

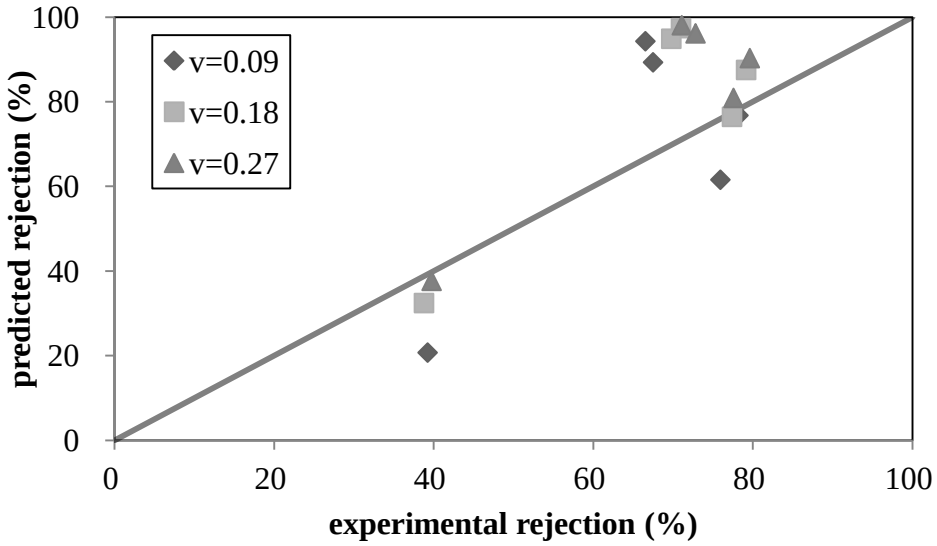

Figure 4-3-8 Predicted rejection versus experimental rejection at different cross flow velocities.

4-3-5-5 Predicted effect of transmembrane pressure

The predicted rejections at various transmembrane pressures at the unity concentration polarization factor for the cross flow velocity of 0.18 m/s are shown in Figure 4-3-9 (a). Rejection increases as transmembrane pressure increases, especially for solutes with a low rejection. Figure 4-3-9 (a) does not account for the concentration polarization effect. Predicted rejections which do consider the concentration polarization effect are shown in Figure 4-3-9 (b). When the concentration polarization effect is considered, rejection at high transmembrane pressure (140 psi) decreases significantly. The concentration polarization factors calculated based on the model for different solutes at various transmembrane pressure are shown in table 4-3-7. At a higher transmembrane pressure, the concentration polarization factor is higher, leading to a rejection decrease. As a result, when transmembrane pressure increases, rejection of solutes increases and then decreases.

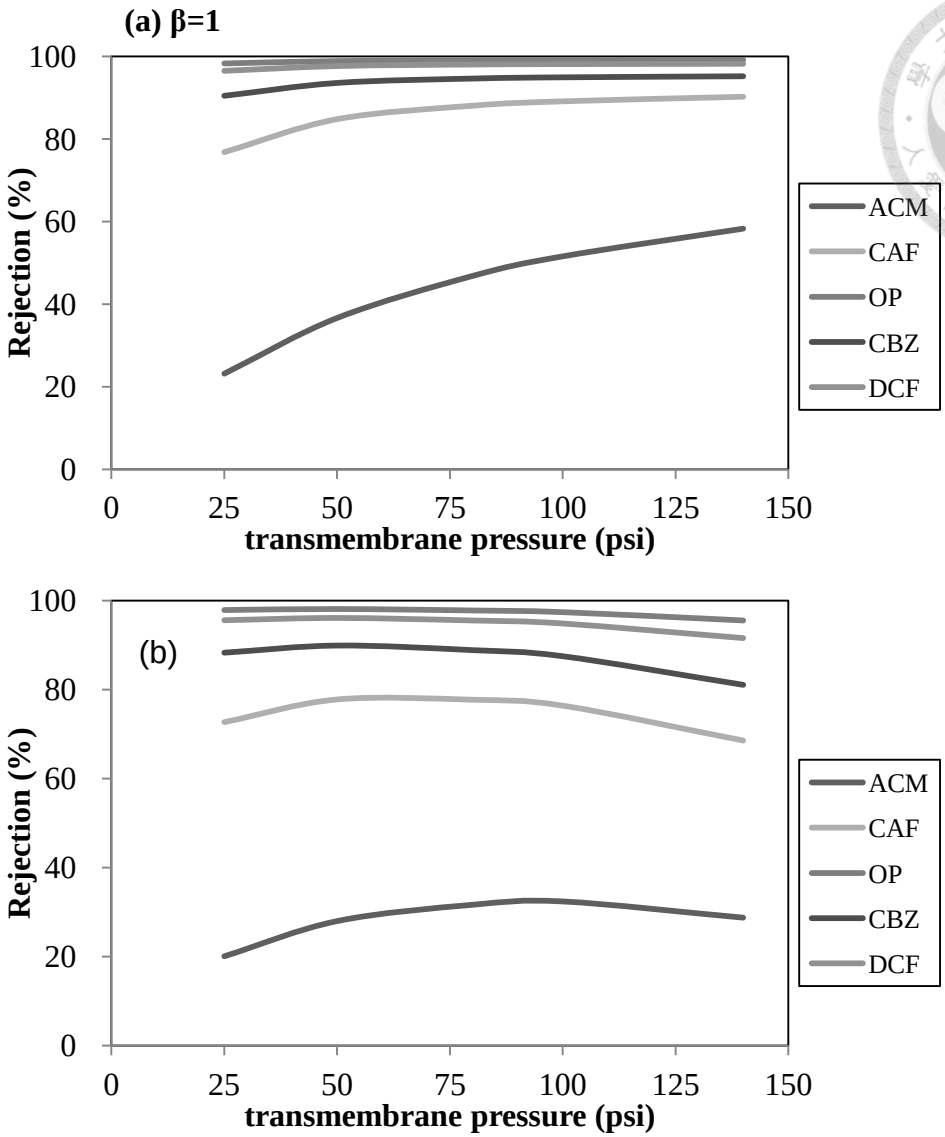

Figure 4-3-9 Predicted rejection at different transmembrane pressures at unity concentration polarization factor (a) or including concentration polarization factor (b) at cross flow velocity 0.18m/s

Table 4-3-7 Concentration polarization factor β at different transmembrane pressures

transmembrane presure (psi)	ACM	CAF	OP	CBZ	DCF
25	1.20	1.24	1.28	1.26	1.28
50	1.49	1.59	1.71	1.64	1.69
80	1.90	2.11	2.37	2.21	2.32
100	2.22	2.53	2.92	2.68	2.84
140	3.46	4.23	5.29	4.64	5.07

The predicted rejection and the experimental rejection under various transmembrane pressures are shown in Figure 4-3-10. Predicted rejection is similar to the experimental rejection for low rejection solute, but deviates from the experimental rejection at high transmembrane pressures. Figure 4-3-11 shows the experimental rejection and predicted rejection without considering concentration polarization and predicted rejection of low rejection solute (acetaminophen) and medium rejection solute (caffeine) at different transmembrane pressures. For the low rejection solute (acetaminophen), experimental rejection is in the middle of the predicted rejection with and without including concentration polarization. For the medium rejection solute (caffeine), experimental rejection is lower than the predicted rejection considering the concentration polarization. As a result, concentration polarization plays some role in rejection, but the extent of it may be lower and need to be adjusted.

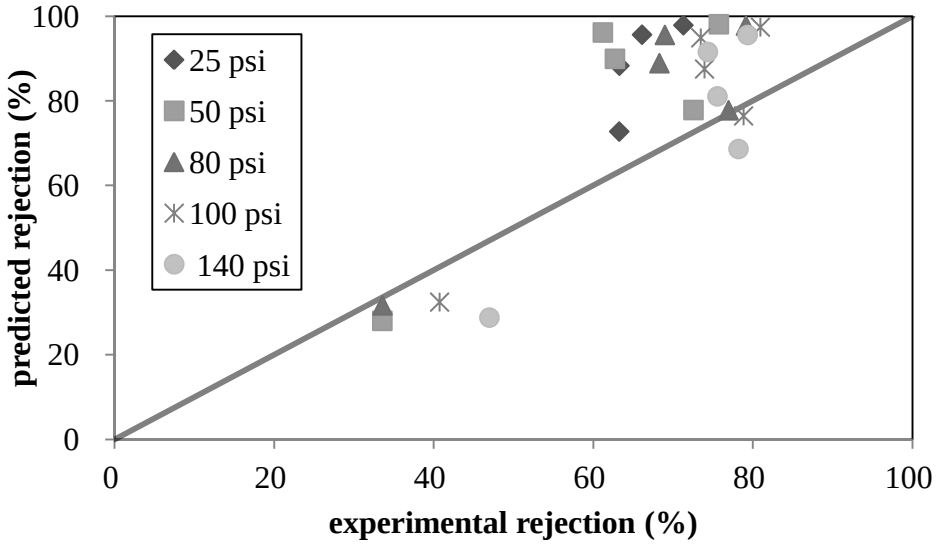

Figure 4-3-10 Predicted rejection versus experimental rejection at transmembrane pressures.

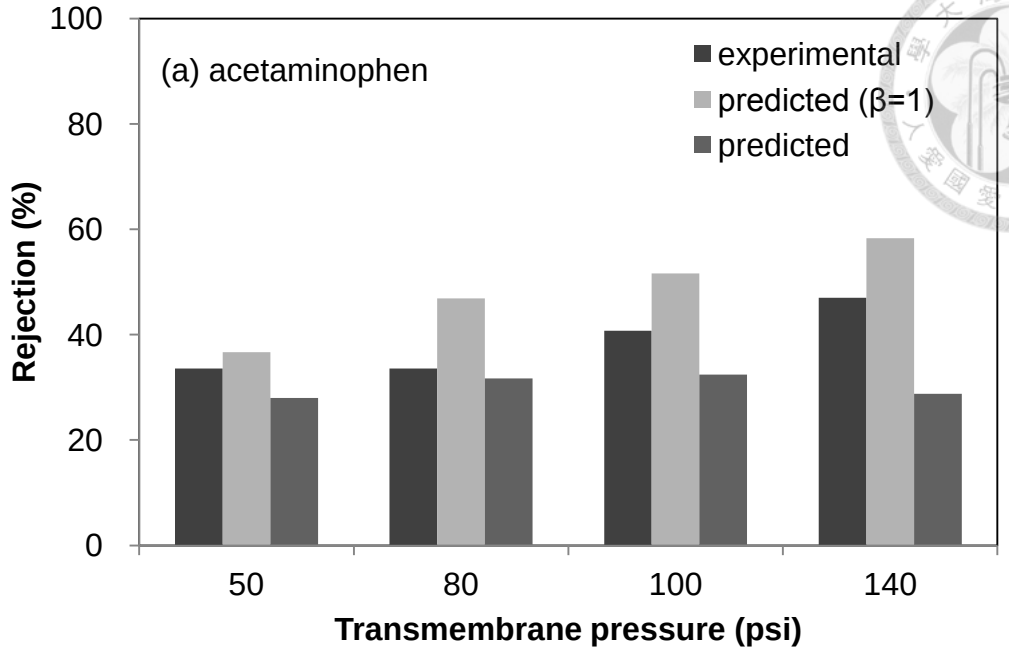

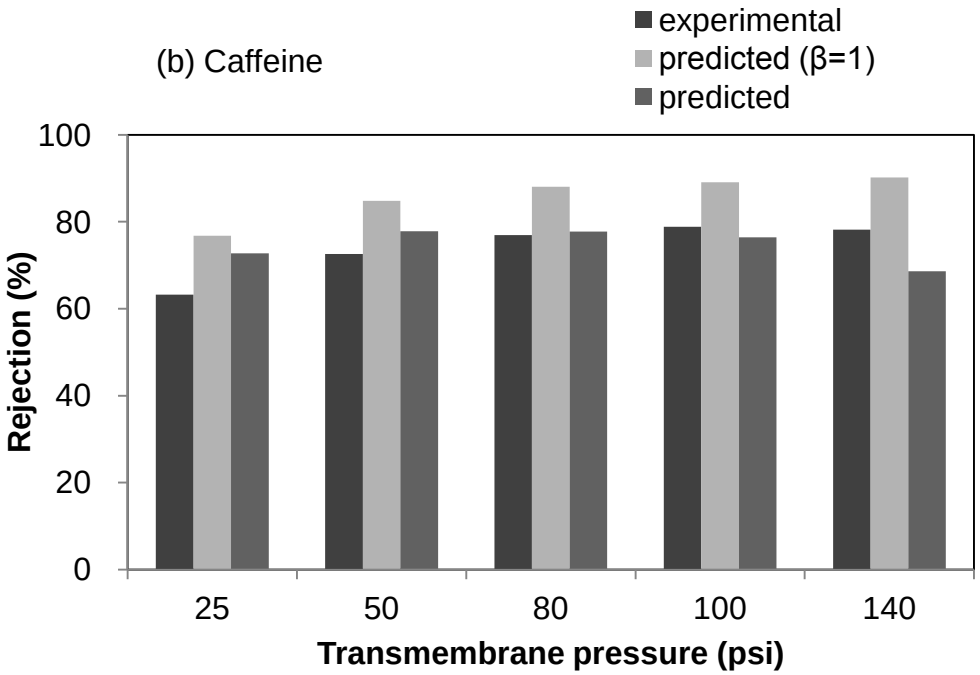

Figure 4-3-11 Compared experimental rejection, predicted rejection not include concentration polarization, and predicted rejection of acetaminophen (a) and caffeine (b) at different transmembrane pressures..

Chapter 5 Conclusions & Recommendations

5-1 Conclusions

1. The experimental results show that the rejection was increased by decreasing membrane pore size or increasing the transmembrane pressure, and the rejection slightly increased by increasing the cross-flow velocity or increasing membrane thickness.
2. Changing the pH, i.e., pH 3 and pH 8 for NF experiments, could validate the hypothesis: G2 exhibits the highest rejection due to electrostatic repulsion; while G1 and G3 are not affected by electrostatic repulsion.
3. The results of the adsorption revealed that G3 and hydrophobic G2 at pH 3 contained adsorption effect. Adsorption will lead to initial rejection higher than final rejection and feed concentration decrease with time. However, adsorption may results in final rejection lower than that of compounds of similar size.
4. Both the irreversible thermodynamics model and the extended Nerst-Plank model could predict the rejections of the small compounds of G1 and G3 such as acetaminophen and caffeine due to size exclusion, but both of them would overestimate the rejections of large compounds. Therefore, the charged extended Nerst-Plank model sould be introduced for G2.
5. The membrane pore size may have important effect on predicted rejection.

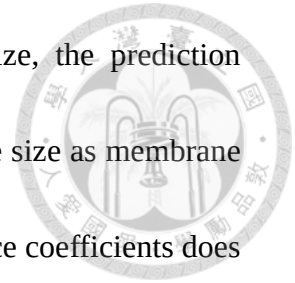

However, because of non-uniform of the membrane pore size, the prediction rejections are overestimated for solutes that are nearly the same size as membrane pore size. Using different calculating methods of steric hindrance coefficients does not vary the rejection.

6. Changing the concentration polarization factor will significantly affect the observed rejection. Changing the cross flow velocity and transmembrane pressure conditions for predicted rejection showed that the concentration polarization factor may play a role on rejection, but value of it may not be calculated correctly.

5-2 Recommendations

1. In this research, error patterns of rejection model were presented. Further revised of rejection model can be conducted in future research.
2. This study was conducted in circular situation. However, in real water treatment, clean water needs to be collected. Thus, it is important for future research to collect permeate water, and discuss the effect of recovery ratio. Also, solvent flux is an important parameter in real water treatment, so the effect on solvent flux can be considered more in future research.
3. For small or hydrophobic solute, the rejection of nanofiltration may be low. So it can be good to combine nanofiltration and activated carbon for water treatment.
4. To elevate the rejection by nanofiltration membrane, the surface-modification of NF membrane can be conducted.
5. Nanofiltration fouling is a problem in water treatment, so it is good for studying the methods of cleaning nanofiltration membrane.

Reference

Bellona, C., Drewes, J. E., Xu, P., Amy, G., 2004. Factors affecting the rejection of organic solutes during NF/RO treatment—a literature review. Water Research 38**,** 2795-2809.

Bowen, W.R., Mohammad, A.W., Hilal, N., 1997. Characterisation of nanofiltration membranes for predictive purposes — use of salts, uncharged solutes and atomic force microscopy. Journal of Membrane Science 126**,** 91-105.

Braeken, L., Bettens, B., Boussu, K., Van De Meeren, P., Cocquyt, J., Vermant, J., Van der Bruggen, B., 2006. Transport mechanism of dissolved organic compound in aqueous solution during nanofiltration. Journal of Membrane Science 279, 311-319.

Bungay, P.M., Brenner, H., 1973. The motion of a closely fitting sphere in a fluid-filled tube. Int. J. Multiph. Flow 1, 25-56.

Comerton, A.M., Andrews, R.C., Bagley D.M., Yang, P., 2007. Membrane adsorption of endocrine disrupting compounds and pharmaceutically active compounds. Journal of Membrane Science 303**,** 267-277.

Darling, E., Litwiller, E., Reinhard, M., 2010. Effects of sorption on the rejection of trace organic contaminants during nanofiltration. Environmental Science and Technology 44, 2592–2598.

Dechadilok, P., Deen, W., 2006. Hindrance factors for diffusion and convection in pores. Industrial Engineering and Chemical Research 45, 6953-6959.

Enick, O.V., Moore, M.M., 2007. Assessing the assessments: Pharmaceuticals in the environment. Environmental Impact Assessment Review 27, 707-729.

Garba, Y., Taha, S., Gondrexon, N., Cabon, J., Dorange, G., 2000. Mechanisms involved in cadmium salts transport through a nanofiltration membrane: characterization and distribution. Journal of Membrane Science 168**,** 135-141.

Huerta-Fontela, M., Galceran, M.T., Ventura, F., 2011. Occurrence and removal of pharmaceuticals and hormones through drinking water treatment. Water Research 45**,** 1432-1442.

Jacangelo, J.G., Trussell, R.R., Watson, M., 1997. Role of membrane technology in drinking water treatment in the United States. Desalination 113**,** 119-127.

Kedem, O., Katchalsky, A., 1958. Thermodynamic analysis of the permeability of biological membranes to non-electrolytes. Biochemica et Biophysica Acta 27, 229-246.

Kim, T.U., Drewes, J.E, Summers, R.S., Amy, G.L., 2007a. Solute transport model for trace organic neutral and charged compounds through nanofiltration and reverse osmosis membranes. Water Research 41**,** 3977-3988.

Kim, Y., Choi, K., Jung, J., Park, S., Kim, P.G., Park, J., 2007b. Aquatic toxicity of

acetaminophen, carbamazepine, cimetidine, diltiazem and six major sulfonamides, and their potential ecological risks in Korea. Environment International 33, 370-375.

Kimura, K., Amy, G., Drewes, J.E., Heberer, T., Kim, T.U., Watanabe, Y., 2003. Rejection of organic micropollutants (disinfection by-products, endocrine disrupting compounds, and pharmaceutically active compounds) by NF/RO membranes. Journal of Membrane Science 227, 113-121.

Kiso, Y., Sugiura, Y., Kitao, T., Nishimura, K., 2001. Effects of hydrophobicity and molecular size on rejection of aromatic pesticides with nanofiltration membranes. Journal of Membrane Science 192, 1-10.

Lin, A.Y.C., Tsai, Y.T., 2009. Occurrence of pharmaceuticals in Taiwan's surface waters: Impact of waste streams from hospitals and pharmaceutical production facilities. Science of The Total Environment 407, 3793-3802.

López-Muñoz, M. J., Sotto, A., Arsuaga, J. M., Van der Bruggen, B., 2009. Influence of membrane, solute and solution properties on the retention of phenolic compounds in aqueous solution by nanofiltration membranes. Separation and Purification Technology 66, 194-201

McCallum, E.A., Hyung, H., Anh Do, T., Huang, C.H., Kim, J.H., 2008. Adsorption, desorption, and steady-state removal of 17 β-estradiol by nanofiltration

membranes. Journal of Membrane Science 319, 38-43.

Murthy, Z.V.P., Gupta, S.K., 1997. Estimation of mass transfer coefficient using a combined nonlinear membrane transport and film theory model. Desalination 109, 39-49.

Nghiem, L.D., Schäfer, A.I., 2004a. Trace Contaminant Removal with Nanofiltration, in: Nanofiltration – Principles and Applications, Schäfer A.I., Waite T.D., Fane A.G. (Eds). Elsevier, Chapter 8, 479-520.

Nghiem, L.D., Schäfer, A.I., Elimelech, M., 2004b. Removal of natural hormones by nanofiltration membranes: Measurement, modeling, and mechanisms. Environmental Science and Technology 38, 1888-1896.

Nghiem, L.D., Schäfer, A.I., Elimelech, M., 2005. Pharmaceutical Retention Mechanisms by Nanofiltration Membranes. Environmental Science and Technology 39, 7698-7705.

Nghiem, L. D., Schäfer, A.I., Elimelech, M., 2006. Role of electrostatic interactions in the retention of pharmaceutically active contaminants by a loose nanofiltration membrane. Journal of Membrane Science 286, 52-59.

Nghiem, L.D., Coleman, P.J., 2008. NF/RO filtration of the hydrophobic ionogenic compound triclosan: Transport mechanisms and the influence of membrane fouling. Separation and Purification Technology 62, 709-716.

Radjenovic, J., Petrovic, M., Ventura, F., Barceló, D., 2008. Rejection of pharmaceuticals in nanofiltration and reverse osmosis membrane drinking water treatment. Water Research 42, 3601-3610.

Spiegler, K.S., Kedem, O., 1966. Thermodynamics of hyperfiltration (reverse osmosis): criteria for efficient membranes. Desalination 1, 311-326.

Van der Bruggen, B., Schaep, J., Wilms, D., Vandecasteele, C., 1999. Influence of molecular size, polarity and charge on the retention of organic molecules by nanofiltration. Journal of Membrane Science 156, 29-41.

Van der Bruggen, B., Vandecasteele, C., 2002. Modelling of the retention of uncharged molecules with nanofiltration.Water Research 36, 5, 1360-1368.

Van der Bruggen, B., Vandecasteele, C., 2003. Removal of pollutants from surface water and groundwater by nanofiltration: overview of possible applications in the drinking water industry. Environmental Pollution 122, 435-445.

Verliefde, A.R.D., Heijman, S.G.J., Cornelissen, E.R., Amy, G., Van der Bruggen, B., van Dijk, J.C., 2007. Influence of electrostatic interactions on the rejection with NF and assessment of the removal efficiency during NF/GAC treatment of pharmaceutically active compounds in surface water. Water Research 41, 3227-3240.

Verliefde, A.R.D., Cornelissen, E.R., Heijman, S.G.J., Verberk, J.Q.J.C., Amy, G.L.,

Van der Bruggen, B., van Dijk, J.C., 2009. Construction and validation of a full-scale model for rejection of organic micropollutants by NF membranes. Journal of Membrane Science 339, 10-20.

Yangali-Quintanilla, V., Sadmani, A., McConville, M., Kennedy, M., Amy, G., 2009. Rejection of pharmaceutically active compounds and endocrine disrupting compounds by clean and fouled nanofiltration membranes. Water Research 43**,** 2349-2362.

Yoon, J., Amy, G., Yoon, Y., 2005. Transport of target anions, chromate, arsenate, and perchlorate through RO, NF, and UF membranes. Water Science Technology 51, 327–334.

Yoon, Y., Westerhoff, P., Snyder, S.A., Wert, E.C., 2006. Nanofiltration and ltrafiltration of endocrine disrupting compounds, pharmaceuticals and personal care products. Journal of Membrane Science 270**,** 88-100.

Appendix

Permeate flow rate and solvent flux for various types of nanofiltration membrane at transmembrane pressure 100 psi, pH 3, and cross flow velocity 0.27 m/s.

	Qp (mL/min)	Jv (10^{-5}m/s)
NF 270	19	2.3
NF 40	8.0	1.0
NF 90	9.0	1.1

The rejection of acetaminophen, caffeine, carbamazepine, diclofenac, and octylphenol by different NF membrane at transmembrane pressure 100 psi, pH 3, and cross flow velocity 0.27 m/s.

	NF 270	NF 40	NF 90
Acetaminophen	40	59	92
Caffieine	73	79	95
Carbamazepine	80	86	95
Diclofenac	58	68	91
Octylphenol	61	71	86

Permeate flow rate and solvent flux operated under various level of transmembrane pressure by NF-270 membrane at pH 3 and cross flow velocity 0.18 m/s.

transmembrane pressure	Qp (mL/min)	Jv (10^{-5}m/s)
140	34.6	4.16
100	23.8	2.86
80	19.0	2.28
50	11.1	1.33

Rejections of mixed solutes by NF-270 membrane operated under various level of transmembrane pressures at pH 8 and cross flow velocity=0.18m/s

transmembrane pressure	ACM (G1)	CAF(G1)	CBZ (G1)	DCF(G2)	OP (G3)
50	31	65	75	93	58
80	35	70	78	94	62
100	41	73	80	94	64
140	48	75	81	94	67

Rejections of mixed solutes by NF-270 membrane operated under various level of transmembrane pressures at pH 3 and cross flow velocity=0.18m/s

transmembrane pressure	ACM (G1)	CAF(G1)	CBZ (G1)	DCF(G2)	OP (G3)
50	26	67	78	59	54
80	30	71	81	66	67
100	42	73	82	70	71
140	56	74	84	73	72

Rejections of mixed solutes by NF-270 membrane operated under various level of cross flow velocities, transmembrane pressure 100 psi, and at pH 8.

	ACM (G1)	CAF(G1)	CBZ (G1)	DCF(G2)	OP (G3)
v=0.09	39	71	78	55	67
v=0.18	39	73	79	60	71
v=0.27	40	73	80	61	71

Rejections of mixed solutes by NF-270 membrane operated under various level of cross flow velocities, transmembrane pressure 100 psi, and at pH 3.

	ACM (G1)	CAF(G1)	CBZ (G1)	DCF(G2)	OP (G3)
v=0.09	33	69	76	93	57
v=0.18	43	73	80	94	64
v=0.27	42	73	79	91	61

Rejections of target compouns by NF-270 membrane at transmembrane pressure of 100 psi, cross flow velocity of 0.27 m/s, and pH 3 and pH 8 and at initial and at final, respectively.

Group	Name	Rejection at pH 8 at initial	Rejection at pH 8 at final	Rejection at pH 3 at initial	Rejection at pH 3 at final
G1	Acetaminophen	42	41	41	42
G1	Caffeine	73	73	73	73
G1	Carbamazepine	77	79	77	80
G1	Trimethoprim	80	80	98	98
G2	Ibuprofen	93	93	30	25
G2	Sulfamethoxazol	95	95	72	72
G2	Diclofenac	89	91	65	58
G3	Octylphenol	74	61	75	61
G3	Bisphenol A	65	55	65	55

Residual concentration ratio on adsorption experiment of mixed compound without NF membrane at pH 3 (a) and with NF270 membrane at pH 8 (b) and pH 3 (c).

		CAF	CBZ	DCF	OP	ACM
pH 8	0	1.00	1.00	1.00	1.00	1.00
	1	1.00	1.00	1.00	0.82	1.00
	5	1.00	0.95	1.00	0.54	1.00
	24	1.00	0.98	1.00	0.39	1.00
	48	1.00	0.98	1.00	0.33	1.00
pH 3	0	1.00	1.00	1.00	1.00	1.00
	1	1.00	1.00	0.87	0.81	1.00
	5	1.00	1.00	0.70	0.65	1.00
	24	1.00	1.00	0.58	0.53	1.00
	48	1.00	1.00	0.53	0.45	1.00
pH 3, Blank	0	1.00	1.00	1.00	1.00	1.00
	1	1.00	1.00	0.95	0.99	1.00
	5	1.00	1.00	0.98	1.00	1.00
	24	1.00	1.00	0.97	1.00	1.00
	48	1.00	1.00	1.00	1.00	1.00